Accepted Manuscript

Discovery of *N*-Indanyl benzamides as potent RORγt inverse agonists

Jinlong Tian, Nannan Sun, Mingcheng Yu, Xianfeng Gu, Qiong Xie, Liming Shao, Jin Liu, Li Liu, Yonghui Wang

PII: S0223-5234(19)30101-1

DOI: https://doi.org/10.1016/j.ejmech.2019.01.082

Reference: EJMECH 11089

To appear in: *European Journal of Medicinal Chemistry*

Received Date: 13 December 2018

Revised Date: 27 January 2019

Accepted Date: 30 January 2019

Please cite this article as: J. Tian, N. Sun, M. Yu, X. Gu, Q. Xie, L. Shao, J. Liu, L. Liu, Y. Wang, Discovery of *N*-Indanyl benzamides as potent RORγt inverse agonists, *European Journal of Medicinal Chemistry* (2019), doi: https://doi.org/10.1016/j.ejmech.2019.01.082.

Graphic Abstract

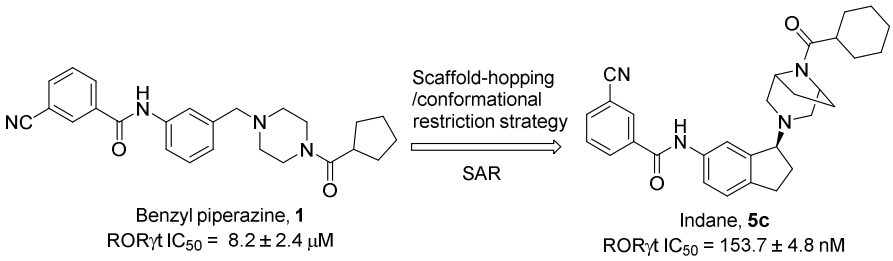

Discovery of *N*-Indanyl Benzamides as Potent RORγt Inverse Agonists

Jinlong Tian[a], Nannan Sun[a], Mingcheng Yu[a], Xianfeng Gu[a], Qiong Xie[a], Liming Shao[a], Jin Liu[b], Li Liu[c,*], Yonghui Wang[a,*]

[a]*Department of Medicinal Chemistry, School of Pharmacy, Fudan University, 826 Zhangheng Road, Shanghai 201203, China*
[b]*Department of Biology and Pharmacology, Shanghai ChemPartner CO., LTD., 998 Halei Road, Shanghai 201203, China*
[c]*State Key Laboratory of New Drug and Pharmaceutical Process, Shanghai Institute of Pharmaceutical Industry, China State Institute of Pharmaceutical Industry, 1111 Zhongshan North No. 1 Road, Shanghai, 200437, China*

*Corresponding authors:

Tel: +86-21-65053962, *E-mail* address: liulisipi@foxmail.com (L. Liu); *Tel:* +86-21-51980118, *E-mail* address: yonghuiwang@fudan.edu.cn (Y. Wang)

Abstract

The retinoic acid receptor-related orphan receptor-gamma-t (RORγt) is a promising therapeutic target for treatment of Th17 cell-mediated autoimmune diseases. Based on a scaffold hopping/conformational restriction strategy, a series of *N*-indanyl benzamides as novel RORγt inverse agonists was discovered. Exploration of structure-activity relationship on the piperazine ring, benzoyl moiety and cyclopentyl moiety of *N*-indanyl benzamides **2a** and **2d** led to identification of potent RORγt inverse agonists. Compound **5c** with (*S*)-enantiomer was found having an IC_{50} of 153.7 nM in Fluorescence Resonance Energy Transfer (FRET) assay, and an IC_{50} of 47.1 nM in mouse Th17 cell differentiation assay, which represents a promising starting point for developing potent small molecule RORγt inverse agonists. Binding modes of the two enantiomers **5c** and **5d** in RORγt ligand binding domain were also discussed.

Keywords: *N*-indanyl benzamides; RORγt inverse agonists; Th17 cells; autoimmune diseases; binding modes

1. Introduction

The retinoic acid receptor-related orphan receptor-gamma-t (RORγt), an isoform of RORγ restrictedly expressed in the thymus, is a key transcriptional factor in Th17 cell differentiation[1-6]. Th17 cells produce inflammatory cytokines (IL-17A, IL-17F, etc.), which play a central role in the pathogenesis of various autoimmune diseases such as psoriasis, rheumatoid arthritis, and multiple sclerosis[7-14]. Recently, accumulated clinical efficacy of the biologics has confirmed importance of the Th17 pathway as a viable clinical target for the treatment of psoriasis, rheumatoid arthritis, ankylosing spondylitis and uveitis[15-20]. Given the crucial role of RORγt in the differentiation of Th17 cells, RORγt has been considered as a promising therapeutic target for treatment of Th17 cell-mediated autoimmune diseases[21].

Since the identification of digoxin[22], SR1001[23] and ursolic acid[24] as small molecule RORγt inhibitors, quite a number of small molecule RORγt inhibitors have been reported[21,25-28]. Among them, a few compounds such as VTP-43742, GSK-2981278, AZD-0284, ESR-114, ARN-6069, AUR-101, RTA-1701 and others have been progressed into clinical trials (Figure 1)[29]. However, some of these front-runners have failed in clinical trials due to compound toxicities or lack of efficacy. Thus, the development of more and better RORγt inhibitors with diverse structure types for therapeutic use remains in need.

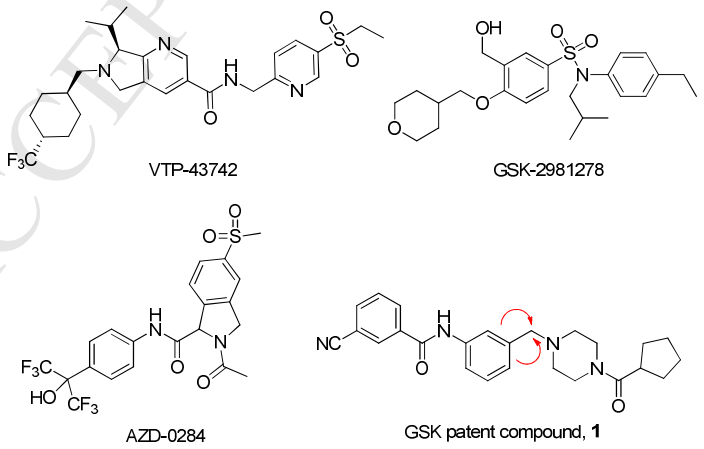

Figure1. Structures of RORγt inhibitors in clinical trials and benzyl piperazine **1**

Previously, we have reported the discovery of RORγt inhibitors such as carbazole carboxamides[30], thiazole/thiophene ketone amides[31], thiazole ether

amides[32], indole amides[33] and biaryl amides[34]. Recently, GlaxoSmithKline (GSK) disclosed a series of benzyl piperazines as novel RORγt inhibitors in their PCT patents[35-38]. Subsequently, a few RORγt inhibitors based on the benzyl piperazine scaffold were disclosed by Pfizer[39], Novartis[40] and LEO Pharm[41]. In light of benzyl piperazine representing a unique structure type and displaying reasonable RORγt activities, it was chosen as our starting scaffold for further structural modification. Compound **1**, a typical GSK patent compound with the benzyl piperazine scaffold, displayed low RORγt activity (IC_{50} of 8.2 μM) in our FRET assay (Figure 1). We hypothesized that cyclization of the benzyl core using a scaffold hopping/conformational restriction strategy could rigidify the molecule and improve its RORγt activity. In this paper, we report the design, synthesis, structure-activity relationship (SAR) of a series of indane-containing compounds as novel RORγt inhibitors. The binding modes of two indane enantiomers in the RORγt ligand binding domain (LBD) were also discussed.

2. Results and discussion

2.1 Compound design

First, the analogs of benzyl piperazine **1** with different bicyclic cores (**2a-2g**) were designed with aid of computer modeling and docking, trying to identify new bicyclic cores that could maintain RORγt inhibitory activity. Then, with the best indane cores (**2a** and **2d**) identified, some compounds with modification on piperazine moiety (**3a-3d** and **4a-4d**) were designed and evaluated. Finally, SARs of left-hand-side (LHS) benzoyl moiety and right-hand-side (RHS) cyclopentyl moiety were investigated on two different indane cores (**5a-5i** and **6a-6g**) to optimize the *N*-indanyl benzamide compounds with better RORγt activity (Figure 2).

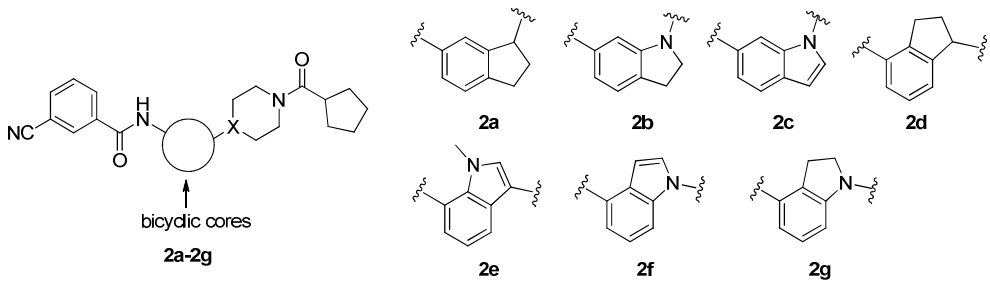

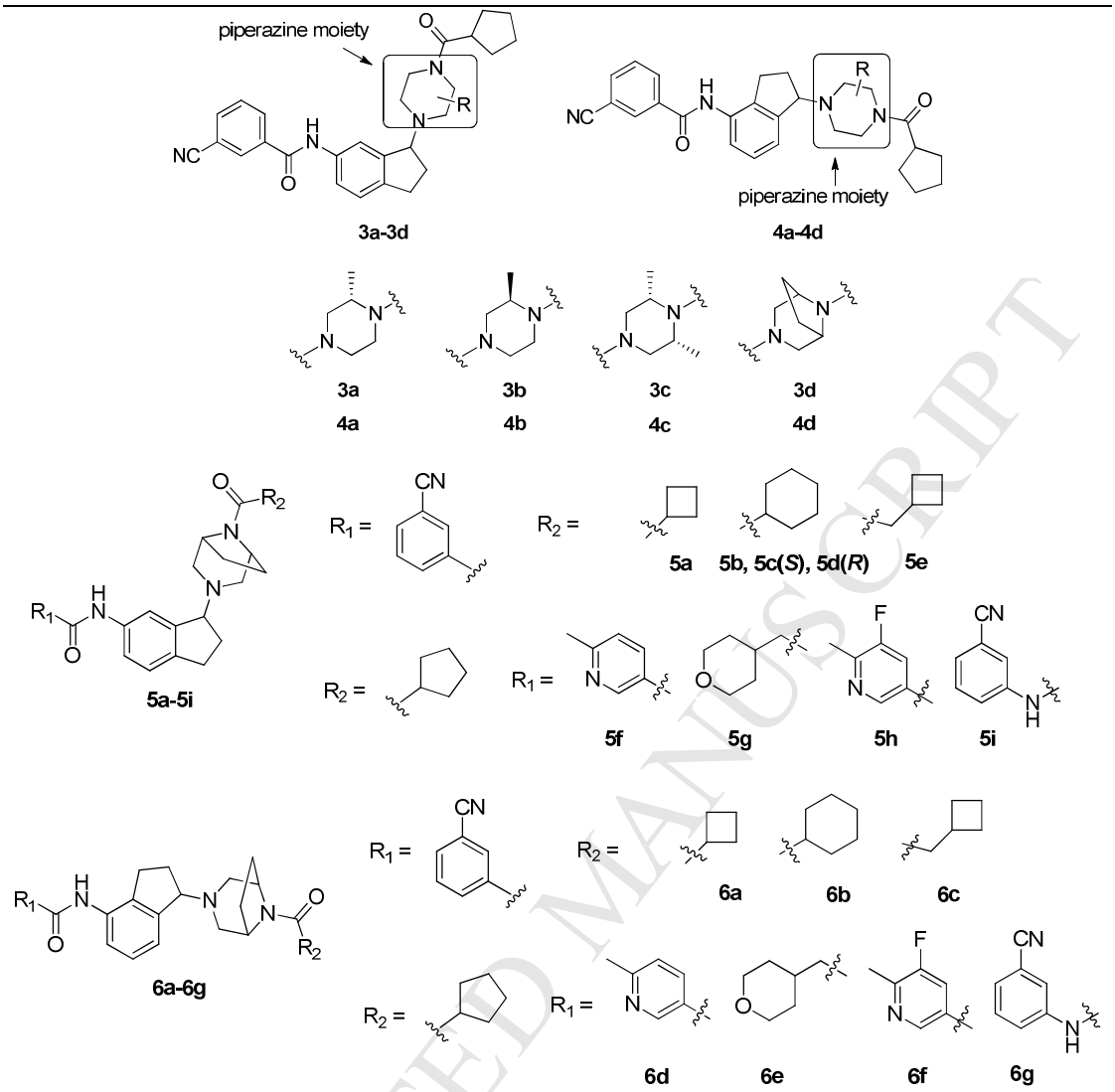

Figure 2. Target compounds with modifications on benzyl core (**2a-g**), piperazine moiety (**3a-d** and **4a-d**), cyclopentyl moiety (**5a-5e** and **6a-6c**) and benzoyl moiety (**5f-5i** and **6d-6g**) of benzyl piperazine **1**

2.2 Chemistry

A general procedure for the synthesis of *N*-indanyl benzamide compounds is described in Scheme 1. The commercially available 1-indanone (**7**) reacted with KNO_3 in the presence of H_2SO_4 to produce compound **8a** or **8b**, which then reacted with Boc-protected piperazine analogues in the presence of sodium cyanoborohydride to obtain compounds **9a** or **9b**. After *N*-deprotection of **9a** or **9b**, the resulting amines subsequently reacted with the corresponding carboxylic acids or acyl chlorides to afford the compounds **10a** or **10b**. Then, the anilines **11a** or **11b** were obtained by the

reduction of the nitro group on **10a** or **10b**. Finally, the target compounds (**2a**, **2d**, **3a-3d**, **4a-4d**, **5a**, **5b**, **5e-5i**, **6a-6g**) were obtained via acylation with the corresponding carboxylic acids or urea formation with anilines/amines. Enantiomers (*S*)-**5c** and (*R*)-**5d** were obtained by chiral HPLC separation of **5b**. The absolute structures of **5c** and **5d** were determined by the optical rotation values of **5c** and **5d** compared with that of (1*R*)-1-Aminoindane in the literature.

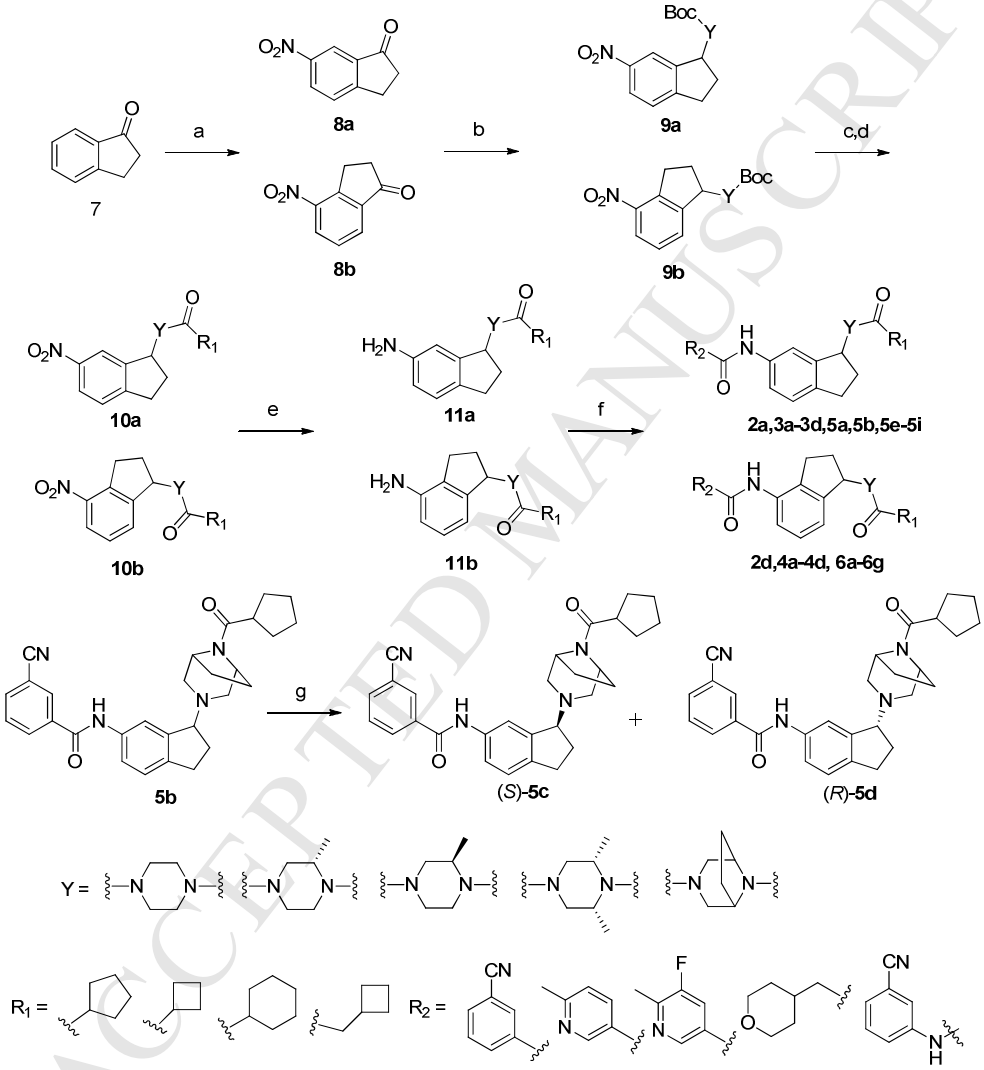

Scheme 1. Synthesis of compounds **2a**, **2d**, **3a-3d**, **4a-4d**, **5a-5i** and **6a-6g**[a]

[a]Reagents and conditions: (a) H_2SO_4, KNO_3, 0□ to rt, 1h; (b) Boc-YH, $NaBH_3CN$, CH_3OH, AcOH, 0□ to rt, overnight; (c) CF_3COOH, DCM, rt, 4h; (d) R_1CO_2H or R_1COCl, DIPEA, DCM, 0□ to rt, 2h; (e) Fe, AcOH, rt, overnight; (f) R_2CO_2H, HATU, DIPEA, DCM, rt, overnight, or *N*-(3-cyanophenyl)-1H-imidazole-1- carboxamide, $ZrCl_4$, THF, reflux; (g) Chiral supercritical-fluid chromatography (SFC), 25% MeOH

(0.2% Methanol ammonia): **5c** (42%), **5d** (56%).

Synthetic procedures of compounds **2b**, **2c**, **2e-2g**, the detailed chiral separation and absolute structure determination of **5c** and **5d** were described in the supporting information.

2.3 Structure-activity relationship

The first set of compounds with different bicyclic cores (**2a-2g**) were designed, synthesized and evaluated in the RORγ FRET assay (Table 1). Cyclization of the methylene carbon of benzyl piperazine **1** to the 4-position of central phenyl ring resulting in indane compound **2a** improved the RORγt potency by 10-fold (830.0 nM in **2a** vs. 8242.0 nM in **1**), while replacing indane ring in **2a** with indoline ring (**2b**) or indole ring (**2c**) lowered the RORγt activity (1574.5 nM in **2b** and 4897.5 nM in **2c**, respectively). Interestingly, when cyclization of the methylene carbon of benzyl piperazine **1** to the 2-position of central phenyl ring, the resulting indane-containing compound **2d** exhibited a 17-fold improvement in RORγt activity (464.9 nM in **2d** vs. 8242.0 nM in **1**). Replacing indane ring in **2d** with *N*-methylindole ring (**2e**) or indoline ring (**2g**) dramatically decreased the activity and replacing with indole ring (**2f**) completely aborted the activity. Thus, the indane compounds **2a** and **2d** which possessed the best RORγt activity among the bicyclic compounds were subject to further optimization.

Table 1. SAR exploration of benzyl core in **1**.

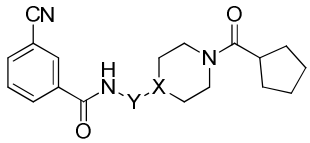

Compd	Y	X	RORγ FRET IC_{50} (nM)[a] (% max. inhibition)[b]
1	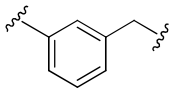	N	8242.0 ± 2387.0 (135.9)
2a	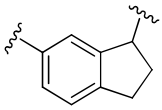	N	830.0 ±19.3 (107.7)

2b	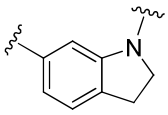	C	1574.5 ± 163.3 (156.2)
2c	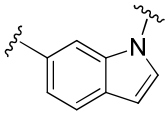	C	4897.5 ± 102.5 (137.8)
2d	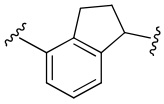	N	464.9 ± 10.1 (149.0)
2e	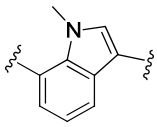	C	6149.0 ± 562.9 (108.7)
2f	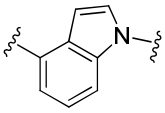	C	N/A[c]
2g	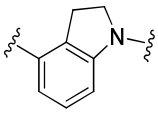	C	5575.0 ± 927.7 (129.7)

[a]IC_{50} value was expressed as mean ± SD, n=2.
[b]Percent max. inhibition measured against activation by the surrogate agonist.
[c]N/A represents no activity.

The SAR of the piperazine moiety of the indanes **2a** and **2d** was then explored, and the results were summarized in Table 2. Replacing the piperazine moiety in **2a** with (*S*)-3-methylpiperazine (**3a**) improved RORγt activity (193.6 nM in **3a** vs. 830.0 ± 19.3 nM in **2a**), while replacing piperazine moiety with (*R*)-3-menthylpiperazine (**3b**) lowered RORγt activity (1674.5 nM in **3b** vs. 830.0 nM in **2a**), indicating the importance of the chirality in methylpiperazine. Subsequently, we replaced the piperazine moiety with (3*S*, 5*R*)-2,6-dimethylpiperazine moiety (**3c**), resulting in equipotent RORγt activity compared to **2a**. Conformation restriction by bridging two methyl groups in **3c** to form **3d** improved the RORγt activity (207.9 nM in **3d** vs. 925.1 nM in **3c**) and the maximum inhibition (147.4% in **3d** vs. 122.3% in **3c**). We used the same strategy to modify the piperazine moiety of the indane **2d** (Table 2). Interestingly, the RORγt inhibitory potency (IC_{50}) and the maximum inhibition (%) of the methyl substituted piperazines (**4a-4d**) were not dramatically affected by the methyl conformation or conformation restriction on piperazine ring, indicating

that the substituent groups on piperazine moiety might play an insignificant role on biological activities of **2d**. For example, compound **4d** exhibited a slightly improved RORγt activity with an IC_{50} of 287.2 nM relative to **2d** with an IC_{50} of 464.9 nM.

Table 2. SAR exploration of the piperazine moieties.

R	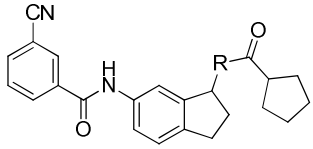		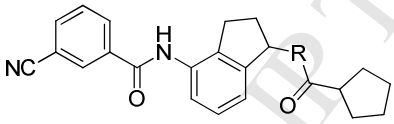	
	Compd	RORγ FRET IC_{50} (nM)[a] (%max.inhibition)[b]	Compd	RORγ FRET IC_{50} (nM)[a] (%max.inhibition)[b]
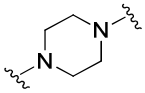	**2a**	830.0 ± 19.3 (107.7)	**2d**	464.9 ± 10.1 (149.0)
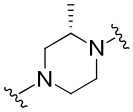	**3a**	193.6 ± 81.9 (118.3)	**4a**	384.7 ± 12.4 (151.8)
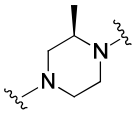	**3b**	1674.5 ± 27.6 (124.0)	**4b**	399.9 ± 68.0 (146.4)
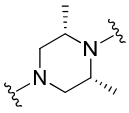	**3c**	925.1 ± 197.8 (122.3)	**4c**	270.3 ± 14.8 (148.9)
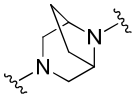	**3d**	207.9 ± 17.9 (147.4)	**4d**	287.2 ± 23.6 (144.3)

[a]IC_{50} value was expressed as mean ± SD, n=2.

[b]Percent max. inhibition measured against activation by the surrogate agonist.

We next explored the SAR of RHS (R_1) and LHS (R_2 and R_3) of the ethylene-bridged piperazines (**3d**) and (**4d**). SAR data were summarized in Tables 3 and 4. Firstly, fixing the R_2 and R_3 moiety as 3-cyano-benzamido, we explored SAR of R_1 in **3d**. Changing the cyclopentyl in **3d** to cyclobutyl (**5a**), cyclohexyl (**5b**) or cyclobutylmethyl (**5e**) could essentially maintain the RORγt activity. Fixing R_1 as cyclopentyl, replacing the LHS 3-cyano-phenyl in **3d** with pyridine derivatives either maintained (**5h**) or mildly decreased (**5f**) the RORγt activity, but with a 4-methyltetrahydro-2*H*-pyran (**5g**), the RORγt activity dropped dramatically, indicating that RORγt activity disfavored non-aromatics in

LHS. Replacing the amide linker in **3d** with a urea linker (**5i**) slightly decreased the RORγt activity. Chiral separation of racemic **5b** led to its two respective enantiomers **5c** and **5d**. The (*S*)-enantiomer **5c** displayed higher RORγt activity compared to **5b** (153.7 nM in **5c** vs. 264.9 nM in **5b**), whereas the (*R*)-enantiomer **5d** displayed no activity at all in the RORγ FRET assay. This result can be explained by the binding mode differences of the compound **5c** and **5d** in RORγt LBD (see section 2.4).

Table 3. SAR explorations of LHS and RHS in **3d**.

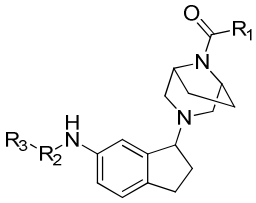

Compd	R_1	R_2	R_3	RORγ FRET IC_{50} (nM)[a] (% Max inhibition)[b]
3d	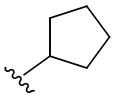		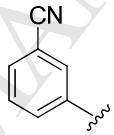	207.9 ± 17.9 (147.4)
5a			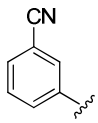	333.2 ± 27.6(141.6)
5b	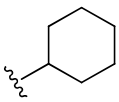		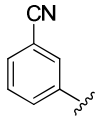	264.9 ± 163.2 (119.2)
5c (*S*)	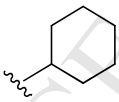		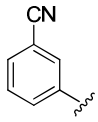	153.7 ± 4.7 (137.3)
5d (*R*)	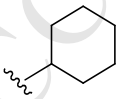		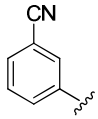	N/A[c]
5e	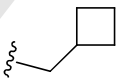		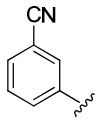	366.7 ± 6.2 (148.9)
5f	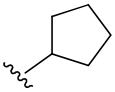		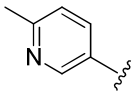	717.9 ± 1.8 (148.1)
5g	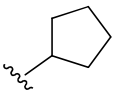		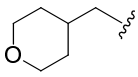	8410.0 ± 1.971.0 (140.1)

5h	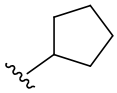		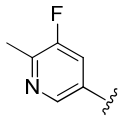	288.4 ± 6.4 (141.5)
5i	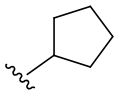	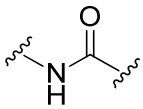	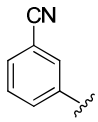	357.7 ± 45.6 (134.2)

[a]IC_{50} value was expressed as mean ± SD, n=2.
[b]Percent max. inhibition measured against activation by the surrogate agonist.
[c]N/A represents no activity.

The SAR of the R_1, R_2 and R_3 in **4d** was explored in a similar way (Table 4). Fixing the R_2 and R_3 moiety as 3-cyano-benzamido, changing the cyclopentyl ring in **4d** with cyclobutyl (**6a**), cyclohexyl (**6b**) or cyclobutylmethyl (**6e**) resulted in a marked drop in RORγt activity. With identification of cyclopentyl as the best RHS substituent in **4d**, we continued to explore the SAR of R_2 and R_3 in LHS. When 3-cyano-phenyl was replaced by either pyridines (**6d** and **6f**) or 4-methyltetrahydro-2*H*-pyran (**6e**), the RORγt activity was greatly reduced. Similarly, replacing the amide linker in **4d** with a urea linker (**6g**) also decreased the RORγt activity.

Table 4. SAR exploration of LHS and RHS in **4d**.

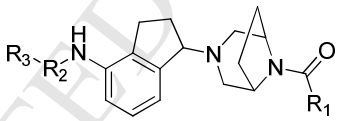

Compd	R_1	R_2	R_3	RORγ FRET IC_{50}(nM)[a] (% Max inhibition)[b]
4d	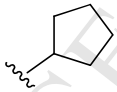		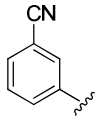	287.2 ± 23.6 (144.3)
6a			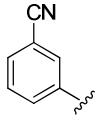	873.4 ± 329.0 (144.3)
6b	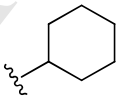		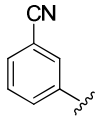	1692.5 ± 415.1 (166.7)
6c	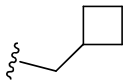		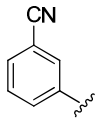	569.3 ± 124.9 (146.4)
6d	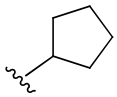		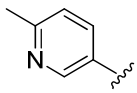	2442.5 ± 466.0 (156.5)

6e	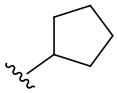		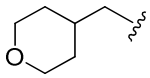	> 10000 (92.8)
6f	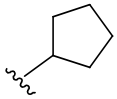		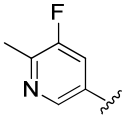	1512.5 ± 352.8 (142.3)
6g	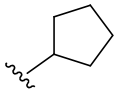	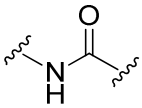	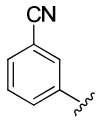	1589.5 ± 1132.0 (114.1)

[a]IC_{50} value was expressed as mean ± SD, n=2.
[b]Percent max. inhibition measured against activation by the surrogate agonist.

We further evaluated the representative *N*-indanyl benzamides **2a**, **2d**, **3d**, **4d**, **5b**-**5d** in the mouse Th17 cell differentiation assay (Table 5). The results revealed that compound **2a** and **2d** containing the piperazine moiety possessed relatively weak Th17 cellular activity. Replacing piperazine ring with ethylene-bridged piperazines (**3d**, **4d** and **5b)** could improve the Th17 cellular activity greatly. Compound **5c** with (*S*)-enantiomer showed excellent activity with an IC_{50} of 47.1 nM in the Th17 cell differentiation assay while the compound **5d** with (*R*)-enantiomer had no activity at all. The activities of the compounds tested in the Th17 cellular assay were essentially consistent with those in the FRET assay.

Table 5. Results in mouse Th17 cell differentiation assay

Compd	mTh17 IC_{50} (nM)[a]
2a	2661.4 ± 2385.2
2d	1782.5 ± 436.3
3d	422.6 ± 39.3
4d	384.6 ± 83.4
5b	105.5 ± 15.9
5c	47.1 ± 4.8
5d	N/A[b]

[a]IC_{50} value was expressed as mean ± SD, n=2.
[b]N/A represents no activity.

2.4 Binding mode study

The activity differences between piperazine ring and ethylene-bridged piperazine ring as well as between the two indane enantiomers such as **5c** and **5d** draw our intention, so docking studies on a few *N*-indanyl benzamide compounds in RORγt

LBD were carried out to understand the mode of actions (MOAs). Docking of **2a** (*S* and *R* enantiomers), **3d** (*S* and *R* enantiomers) and **5b** (**5c** and **5d**) into RORγt LBD revealed the binding mode of a typical indane-based RORγt inverse agonist, which was similar to the reported indole benzamide's binding mode[39]. As illustrated in Figure 3A, in the LHS of *N*-indanyl benzamide **5c**, the benzoyl moiety provides preferred π-π cluster interactions with His323 and Phe377, and the cyano substituent can form a hydrogen bond with the backbone Leu287. The linker amide beside the indane core can form hydrogen bond interaction with the backbone of Phe377. In the RHS of **5c**, the cyclohexyl ring occupies an existed vacant cavity between H11 and H11', and formed intermolecular interactions with surrounding hydrophobic residues in the hydrophobic site near His479. Overlay of **5c** with the reported indole benzamide co-crystal structure in RORγt LBD (PDB ID: 6CN6) reveals a similar overall binding mode (Figure 3B).

Besides the common binding mode, it was also noted that a key hydrogen bond between His479 and the carbonyl group in the RHS of all indane (*S*)-enantiomers is associated with the inverse agonism of RORγt. In the binding modes of (*S*)-enantiomers of **2a**, **3d** and **5b**, the carbonyl group was apt to form hydrogen bonds with His479, breaking the hydrogen bond of His479 and Tyr502, thus made the H11-H12 bridging force weak (Figure 4A). The loose interaction within the triplet residues His479-Tyr502-Phe506 resulted in the disorder of H12, and the unwinding H12 could not recruit co-activator, making these compounds as RORγt inverse agonists. On the contrary, in the binding modes of (*R*)-enantiomers of **2a**, **3d** and **5b**, the carbonyl group is not easily to form hydrogen bond with His479, which might be the reason why (*S*)-enantiomer **5c** is quite active but the (*R*)- enantiomer **5d** not.

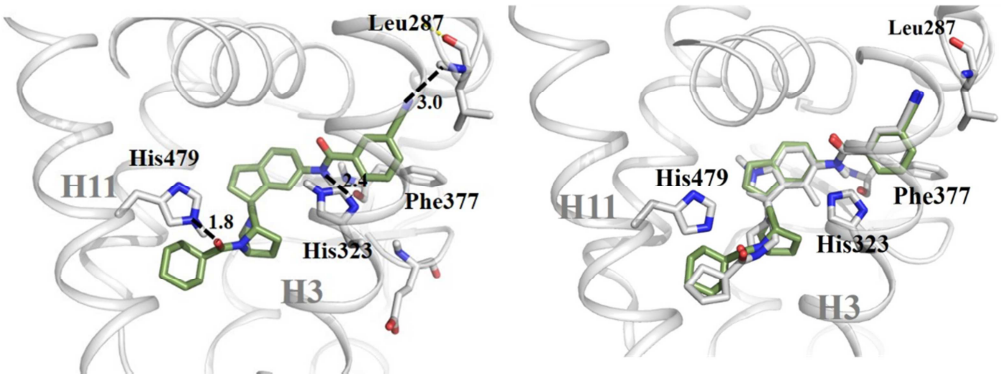

A B

Figure 3. Binding mode of indane derivative **5c**. A: Zoomed-in view of **5c** (shown in

lime) in the binding pocket of RORγt LBD; B: overlay of **5c** with the reported indole benzamide in co-crystal structure (shown in white, PDB ID: 6CN6).

Another note from the binding mode study is that the confirmation of the piperazine moiety constrained by the ethylene bridge can enhance the formation of hydrogen-bond between the carbonyl group and His479 (Figure 4B). Thus, **3d** (*S*)-enantiomer is more preferred to form hydrogen bond with His479 than **2a** (*S*)-enantiomer, which is critical for the secondary structure of H12 as mentioned above. The conformational restriction of the bridged piperazines such as in **3d** is reflected in an activity enhancement as observed not only in the RORγ FRET assay but also in the mouse Th17 cell differentiation assay.

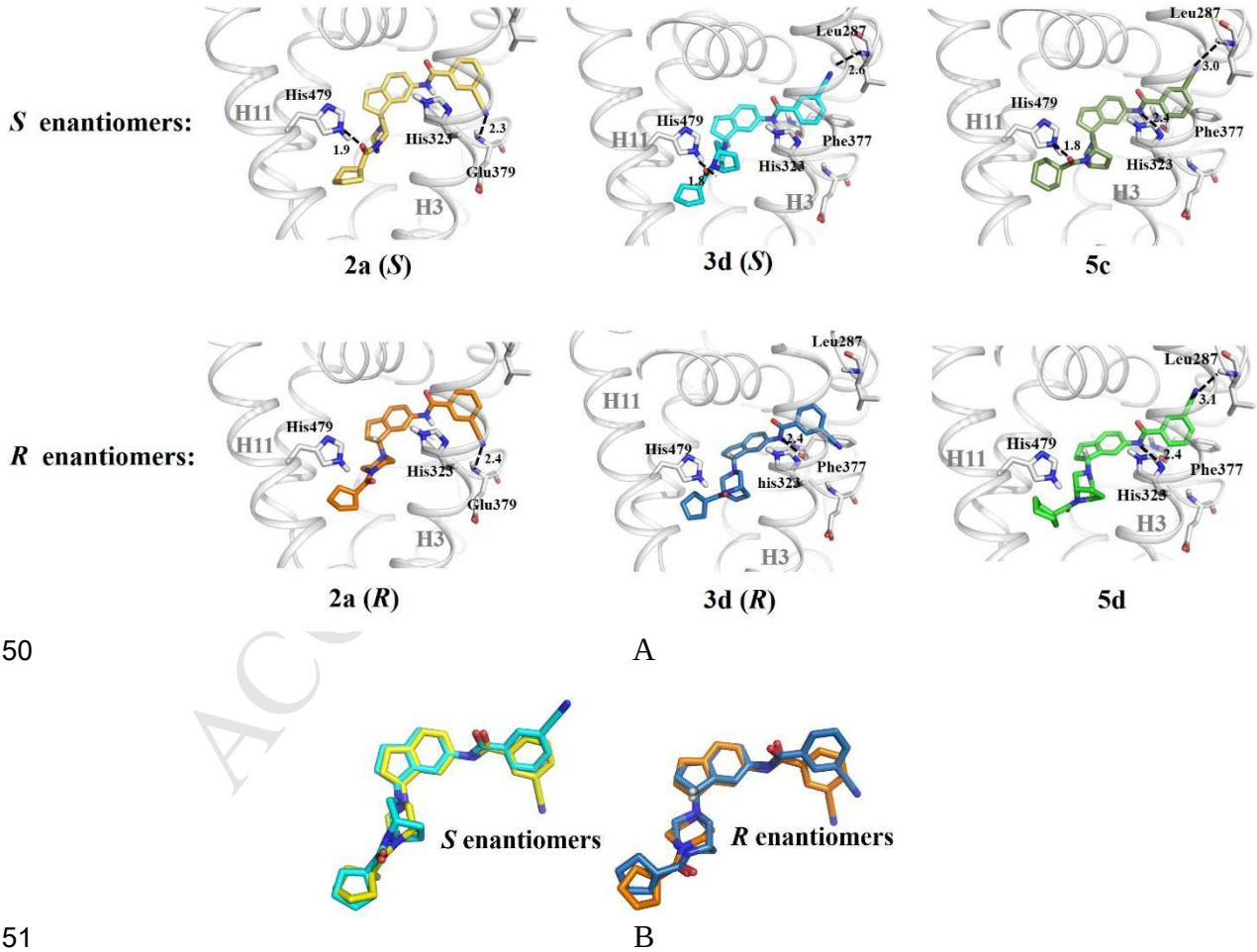

Figure 4. Binding modes of *S* and *R* enantiomers. A: Binding modes of **2a**, **3d** and **5b**; B: overlay of (*S*)-enantiomers of **2a** and **3d**, and (*R*)-enantiomers of **2a** and **3d.** (**2a** (*S*)-enantiomer colored in yellow, **2a** (*R*)-enantiomer colored in orange, **3d**

(*S*)-enantiomer colored in cyan, **3d** (*R*)-enantiomer colored in blue, **5c** colored in lime, **5d** colored in green)

3. Conclusions

In summary, we discovered a series of *N*-indanyl benzamides as novel RORγt inhibitors through cyclization of the benzyl piperazines using a scaffold hopping /conformational restriction strategy. The exploration of structure-activity relationship on the benzyl core, the piperazine ring, the LHS aryl and the RHS cyclopentyl of the benzyl piperazine **1** led to the identification of potent RORγt inhibitors. The indane compound **5c** with (*S*)-enantiomer was found having decent RORγt inhibitory activity with an IC_{50} of 153.7 nM in RORγ FRET assay and 47.1 nM in mouse Th17 cell differentiation assay, and represented a promising starting point for developing potent small molecule RORγt inverse agonists with the potential for treatment of autoimmune diseases. The binding mode study of the *N*-indanyl benzamides in RORγt LBD using a molecular docking method revealed the rationales that why the bridged piperazines are more potent than piperazine and the (*S*)-enantiomer compared to (*R*)-enantiomer was preferred in RORγt activity. Further optimization of the *N*-indanyl benzamide lead series is ongoing and will be reported in due course.

4. Experimental

4.1. Materials and methods

All the reagents used were commercially available and were used without further purification unless otherwise indicated. All of the reactions were monitored by thin layer chromatography (TLC) using silica gel plates (fluorescence F254, UV light). The intermediate and the final target compound was purified by column chromatography on silica gel 200~300 GF254 (Qingdao Haiyang Chemical Co., Ltd., Qingdao, Shandong Province, China). Melting point was recorded by WRS-1B digital instrument. ^{1}H NMR spectra was recorded on a Bruker 400 MHz spectrometer, Coupling constants (*J* values) were given in hertz (Hz). ^{13}C NMR spectra was recorded at 600 MHz. Chemical shifts (δ) were reported in parts per million (ppm)

(using TMS as an internal control). Signals were described as singlet (s), doublet (d), triplet (t), quartet (q), multiplet (m), and broad (br). Mass spectroscopy was carried out on Electrospray ionization (ESI) instruments or MALDI-TOF (Bruker).

4.2. Synthesis

*4.2.1. General procedure for the synthesis of indane analogues (**2a**, **2d**, **3a-3d**, **4a-4d**, **5a-5i** and **6a-6g**)*

Step 1: To a solution of 2,3-dihydro-1H-inden-1-one (1.0 eq) in sulfuric acid stirred at $0^{o}C$ was added KNO_3 (1.05 eq) in several portions over 15 mins and the reaction mixture was stirred for 1 hr at this temperature. After the reaction completed, the mixture was poured into ice-water, and extracted with AcOEt. The organic phase was washed with water and saturated $NaHCO_3$ solution, dried over anhydrous sodium sulfate, filtered and the filtrate was concentrated under reduced pressure to afford the crude product, which was purified by column chromatography (silica gel, eluent: AcOEt/Pet 0-25%, v/v) to give the 6-nitro-2,3-dihydro-1H-inden-1-one intermediate **8a** and 4-nitro-2,3-dihydro-1H-inden-1-one intermediate **8b**.

Step 2: To a solution of 6-nitro-2,3-dihydro-1H-inden-1-one intermediate **8a** (1.0 eq) or 4-nitro-2,3-dihydro-1H-inden-1-one intermediate **8b** (1.0 eq) and Boc-protection piperazine analogues (1.5 eq) in methanol was added acetic acid (1.5 eq) and $NaBH_3CN$ (2.0 eq) at room temperature and the reaction mixture was heated to reflux overnight. When the starting material was consumed completely, the mixture was cooled to room temperature, and saturated NH_4Cl solution was added to the mixture to quench the reaction. The mixture was concentrated under reduced pressure and extracted with AcOEt. The organic phase was washed with water and saturated $NaHCO_3$ solution, dried over anhydrous sodium sulfate, filtered and the filtrate was concentrated under reduced pressure to afford the crude product, which was purified by column chromatography (silica gel, eluent: PE/DCM 0-50%, v/v) to give the 6-nitro-indanyl analogue **9a** or 4-nitro-indanyl analogue **9b**.

Step 3: To a solution of 6-nitro-indanyl analogue **9a** (1.0 eq) or 4-nitro-indanyl analogue **9b** (1.0 eq) in DCM (4 mL) was added trifluoroacetic acid (2.0 mL) at $0^{o}C$

and the reaction mixture was stirred at this temperature for 3 hours. When the starting material was consumed completely, the mixture was concentrated under reduced pressure to remove the solvent. The resulting residue was dissolved with DCM and Et_3N (3.0 eq). Different acid chloride (1.05 eq) was dropwise to the mixture for 10min. Then the reaction mixture was stirred for another 1 hour. Methanol was added to the reaction mixture to quench the reaction. The mixture was concentrated under reduced pressure to remove the solvent. The crude product was purified by column chromatography (silica gel, eluent: PE/DCM 0-100%, v/v) to give the compound **10a** or compound **10b**.

Step 4: To a solution of compound **10a** (1.0 eq) or compound **10b** (1.0 eq) in methanol (5.0 mL) was added Pd/C (5%, 0.2 eq, M/M) at room temperature under H_2 atmosphere and the reaction mixture was stirred at this temperature overnight. When the starting material was consumed completely, the mixture was filtered and the filtrate was concentrated under reduced pressure to to give the crude compound **11a** or compound **11b** which was used directly in the next step.

Step 5a: The mixture of the crude compound **11a** (1.0 eq) or compound **11b** (1.0 eq), HATU (1.5 eq), different acid (1.1 eq) and DIPEA (3.0 eq) in DCM was stirred at room temperature overnight under N_2 atmosphere. When the starting material was consumed completely, the mixture was washed with saturated $NaHCO_3$ solution and water, dried over anhydrous sodium sulfate, filtered and the filtrate was concentrated under reduced pressure to afford the crude product, which was purified by column chromatography to afford the target compounds (**2a**, **2d**, **3a-3d**,**4a-4d**, **5a**, **5b**, **5e-5h** and **6a-6f**). Enantiomers (*S*)-**5c** and (*R*)-**5d** were obtained by chiral HPLC separation of **5b**.

Step 5b: The mixture of the crude compound **11a** (1.0 eq) or compound **11b** (1.0 eq), $ZrCl_4$ (1.0 eq), *N*-(3-cyanophenyl)-1H-imidazole-1- carboxamide (1.2 eq) in THF was heated to reflux and stirred at this temperature for 8 hour under N_2 atmosphere. When the starting material was consumed completely, the reaction mixture was filtered and the filtrate was concentrated under reduced pressure, the resulting residue was

purified by flash column chromatography on silica gel to afford the desired product (**5i** and **6g**).

4.2.1.1

*3-Cyano-N-(3-(4-(cyclopentanecarbonyl)piperazin-1-yl)-2,3-dihydro-1H inden -5-yl) benzamide(**2a**)* as white solid (55.4%); mp 229.6-230.4°C. ^{1}H NMR (400 MHz, DMSO-d_6) δ 10.38 (s, 1H), 8.41 (s, 1H), 8.25 (d, *J* = 8.0 Hz, 1H), 8.06 (d, *J* = 7.7 Hz, 1H), 7.80-7.73 (m, 2H), 7.63 (d, *J* = 8.2 Hz, 1H), 7.22 (d, *J* = 8.1 Hz, 1H), 4.34 (t, *J* = 6.9 Hz, 1H), 3.48 (m, 3H), 3.42 (m, 1H), 2.94 (m, 1H), 2.84 (m, 1H), 2.73 (m, 1H), 2.45 (m, 2H), 2.34 (m, 2H), 2.01 (q, *J* = 7.1 Hz, 2H), 1.73-1.49(m, 8H). ^{13}C NMR (151 MHz, DMSO-d_6) δ 173.11, 163.21, 142.74, 139.14, 136.97, 135.85, 134.71, 132.33, 131.08, 129.64, 124.37, 119.80, 118.19, 116.92, 111.32, 69.00, 48.47, 47.98, 45.23, 41.53, 29.76, 29.44, 29.40, 25.49, 24.13. MS (ESI) m/z: 443.3[M+H]$^{+}$. HRMS (ESI^{+}) m/z calcd for $C_{27}H_{30}N_4O_2$ [M+H]$^{+}$: 443.2442; found: 443.2445.

4.2.1.2

*3-Cyano-N-(1-(4-(cyclopentanecarbonyl) piperazin-1-yl)-2,3-dihydro-1H-inden -4-yl) benzamide(**2d**)* as white solid (35.6%); mp 78.5-80.5°C. ^{1}H NMR (400 MHz, DMSO-d_6) δ 10.14 (s, 1H), 8.39 (s, 1H), 8.24 (d, J = 7.6 Hz, 1H), 8.08 (d, J = 7.1 Hz, 1H), 7.75 (t, J = 8.7 Hz, 1H), 7.36 (d, J = 6.6 Hz, 1H), 7.25 (t, J = 7.1 Hz, 1H), 7.18 (d, J = 6.8 Hz, 1H), 4.37 (m, 1H), 3.49 (m, 2H), 2.89 (m, 2H), 2.74 (m, 1H), 2.38 (m, 4H), 1.98 (m, 2H), 1.61 (m, 10H). ^{13}C NMR (151 MHz, DMSO-d_6) δ 173.10, 163.12, 143.61, 138.27, 135.46, 134.82, 133.75, 132.36, 131.22, 129.68, 126.45, 123.19, 122.10, 118.16, 111.39, 69.17, 48.62, 47.95, 45.21, 41.50, 29.43, 28.57, 25.48, 23.66. MS (ESI) m/z: 443.2[M+H]$^{+}$. HRMS (ESI^{+}) m/z calcd for $C_{27}H_{30}N_4O_2$ [M+H]$^{+}$: 443.2442; found: 443.2434.

4.2.1.3

*3-Cyano-N-(3-((S)-4-(cyclopentanecarbonyl)-3-methylpiperazin-1-yl)-2,3-dihydro -1H -inden-5-yl) benzamide (**3a**)* as white solid (45.2%); mp 114.2-115.6°C. ^{1}H NMR (400 MHz, DMSO-d_6) δ 10.39 (s, 1H), 8.40 (d, *J* = 10.0 Hz, 1H), 8.24 (t, *J* = 7.8 Hz,

1H), 8.06 (d, *J* = 7.8 Hz, 1H), 7.81-7.73 (m, 2H), 7.67-7.53 (m, 1H), 7.21 (d, *J* = 7.3 Hz, 1H), 4.54 (m, 1H), 4.35-4.17 (m, 2H), 3.77 (m, 1H), 3.29-3.13 (m, 1H), 2.86 (m, 2H), 2.73 (m, 2H), 2.38-2.15 (m, 2H), 1.99 (s, 2H), 1.69-1.49(m, 8H), 1.35-1.13(m, 3H). ^{13}C NMR (151 MHz, DMSO-d_6) δ 173.13, 163.28, 142.97, 138.98, 136.97, 135.89, 134.69, 132.34, 131.08, 129.63, 124.34, 119.70, 118.18, 116.89, 111.32, 68.97, 54.61, 51.04, 46.59, 43.98, 40.63, 36.60, 29.52, 25.47, 24.07, 16.88, 15.35. MS (ESI) m/z: 457.3[M+H]$^+$. HRMS (ESI$^+$) m/z calcd for $C_{28}H_{32}N_4O_2$ [M+H]$^+$: 457.2598; found: 457.2606.

4.2.1.4

*3-Cyano-N-(3-((R)-4-(cyclopentanecarbonyl)-3-methylpiperazin-1-yl)-2,3-dihydro-1H -inden-5-yl)benzamide(**3b**)* as white solid (30.2%); mp 178.3-179.4°C.^{1}H NMR (400 MHz, DMSO-d_6) δ 10.39 (s, 1H), 8.40 (d, *J* = 10.0 Hz, 1H), 8.24 (t, *J* = 7.4 Hz, 1H), 8.06 (d, *J* = 7.4 Hz, 1H), 7.81 (s, 1H), 7.75 (t, *J* = 7.5 Hz, 1H),7.68-7.53 (m, 1H), 7.21 (d, *J* = 7.1 Hz, 1H), 4.54 (m, 1H), 4.35-4.16 (m, 2H), 3.77 (m, 1H), 3.26 (m, 1H), 2.86 (m, 2H), 2.73 (m, 2H), 2.34-2.19 (m, 2H), 1.98 (s, 2H), 1.69-1.49 (m, 8H), 1.33-1.13 (m, 3H). ^{13}C NMR (151 MHz, DMSO-d_6) δ 173.07, 163.28, 142.98, 138.91, 137.01, 135.96, 134.68, 132.34, 131.08, 129.63, 124.32, 119.70, 118.18, 116.77, 111.33, 68.97, 51.04, 47.83, 46.59, 43.75, 40.64, 30.52, 29.52, 29.05, 25.46, 20.02, 16.81, 15.23. MS (ESI) m/z: 457.3[M+H]$^+$. HRMS (ESI$^+$) m/z calcd for $C_{28}H_{32}N_4O_2$ [M+H]$^+$: 457.2598; found: 457.2599.

4.2.1.5

*3-Cyano-N-(3-((3S,5R)-4-(cyclopentanecarbonyl)-3,5-dimethylpiperazin-1-yl)-2,3-dih -ydro-1H-inden-5-yl)benzamide(**3c**)* as white solid (46.7%); mp 184.7-185.8°C. ^{1}H NMR (400 MHz, DMSO-d_6) δ 10.39 (s, 1H), 8.39 (s, 1H), 8.24 (d, J = 7.4 Hz, 1H), 8.06 (d, J = 7.5 Hz, 1H), 7.84 (s, 1H), 7.75 (t, J = 7.7 Hz, 1H), 7.61 (d, J = 8.1 Hz, 1H), 7.21 (d, J = 8.0 Hz, 1H), 4.37 (m, 2H), 4.09 (m, 1H), 2.85 (m, 2H), 2.72 (m, 2H), 2.42 (m, 1H), 2.32 (m, 2H), 2.08 – 1.94 (m, 2H), 1.78 – 1.49 (m, 8H), 1.38-1.19 (m, 6H).. ^{13}C NMR (151 MHz, DMSO-d_6) δ 174.00, 163.29, 138.94, 137.05, 135.96, 134.69, 132.35, 131.08, 129.63, 124.33, 119.73, 118.18, 116.80, 111.33, 69.29, 55.38, 50.77,

30.52, 29.59, 25.60. MS (ESI) m/z: 471.3[M+H]$^+$. HRMS (ESI$^+$) m/z calcd for $C_{29}H_{34}N_4O_2$ [M+H]$^+$:471.2755; found:471.2750.

4.2.1.6

*3-Cyano-N-(3-(8-(cyclopentanecarbonyl)-3,8-diazabicyclo [3.2.1] octan-3-yl)-2,3-dihydro-1H-inden-5-yl) benzamide(**3d**)* as white solid (66.7%); mp 105.6-106.2°C. ^{1}H NMR (400 MHz, DMSO-d_6) δ 10.38 (s, 1H), 8.39 (s, 1H), 8.24 (d, J = 8 Hz, 1H), 8.06 (d, J = 8 Hz, 1H), 7.75 (m, 2H), 7.59 (d, J = 8 Hz, 1H), 7.19 (d, J = 8 Hz, 1H), 4.48 (m, 1H), 4.34 (m, 2H), 2.78-2.69 (m, 4H), 2.29 (m, 2H), 1.97 (m, 5H), 1.72-1.50 (m, 10H). ^{13}C NMR (151 MHz, DMSO-d_6) δ 170.91, 163.33, 143.00, 138.79, 137.11, 135.99, 134.69, 132.35, 131.10, 129.63, 124.32, 119.61, 118.19, 116.61, 111.33, 68.08, 55.68, 54.09, 51.36, 40.79, 29.77, 29.62, 28.39, 28.24, 26.70, 26.58, 25.64, 24.09, 23.90. MS (ESI) m/z: 469.3[M+H]$^+$. HRMS (ESI$^+$) m/z calcd for $C_{29}H_{32}N_4O_2$ [M+H]$^+$: 469.2598; found:469.2597.

4.2.1.7

*3-Cyano-N-(1-((S)-4-(cyclopentanecarbonyl)-3-methylpiperazin-1-yl)-2,3-dihydro-1H -inden-4-yl)benzamide(**4a**)* as yellow solid (46.9%); mp 103.6-105.8°C.^{1}H NMR (400 MHz, DMSO-d_6) δ 10.14 (s, 1H), 8.39 (s, 1H), 8.24 (d, J = 8.0 Hz, 1H), 8.08 (d, J = 7.6 Hz, 1H), 7.75 (t, J = 8.0 Hz, 1H), 7.36 (d, J = 5.5 Hz, 1H), 7.26 (t, J = 7.6 Hz, 1H), 7.22-7.15 (m, 1H), 4.57-4.51 (m, 1H), 4.42-4.32 (m, 1H), 4.26-4.16 (m, 1H), 3.81-3.70 (m, 1H), 3.33-3.13 (m, 1H), 2.95-2.81 (m, 2H),2.77- 2.67 (m, 2H), 2.44-2.15 (m, 2H), 1.96 (m, 2H), 1.69-1.50 (m, 8H), 1.35-1.06 (m, 3H). ^{13}C NMR (151 MHz, DMSO-d_6) δ 173.13, 163.12, 143.81, 138.08, 135.46, 134.82, 133.75, 132.36, 131.21, 129.68, 126.48, 123.15, 122.03, 118.16, 111.39, 69.12, 50.96, 49.78, 47.77, 43.71, 30.53, 30.31, 29.42, 29.04, 28.53, 28.40, 25.56, 25.46. MS (ESI) m/z: 457.3[M+H]$^+$. HRMS (ESI$^+$) m/z calcd for $C_{28}H_{32}N_4O_2$ [M+H]$^+$: 457.2598; found:457.2589.

4.2.1.8

*3-Cyano-N-(1-((R)-4-(cyclopentanecarbonyl)-3-methylpiperazin-1-yl)-2,3-dihydro-1H -inden-4-yl)benzamide(**4b**)* as yellow solid (28.5%); mp 91.9-92.4°C.^{1}H NMR (400

MHz, DMSO-d_6) δ 10.15 (s, 1H), 8.39 (s, 1H), 8.26 (m, 1H), 8.09 (m, 1H), 7.76 (m, 1H), 7.36 (m, 1H), 7.26-7.17 (m, 2H), 4.56 (m, 1H), 4.37 (m, 1H), 4.19 (m, 1H), 3.83-3.70 (m, 1H), 3.31-3.10 (m, 1H), 2.89 (m, 2H), 2.75 (m, 2H), 2.27(m, 2H), 1.98 (m, 2H), 1.70-1.57 (m, 8H), 1.35-1.12 (m, 3H). ^{13}C NMR (151 MHz, DMSO-d_6) δ 173.12, 163.13, 143.88, 138.15, 135.46, 134.82, 133.75, 132.36, 131.21, 129.68, 126.48, 123.17, 121.73, 118.16, 111.39, 69.23, 50.39, 47.77, 46.63, 43.98, 30.52, 29.04, 28.53, 25.56, 23.49, 22.85, 16.73, 15.36. MS (ESI) m/z: 457.3[M+H]$^+$. HRMS (ESI$^+$) m/z calcd for $C_{28}H_{32}N_4O_2$ [M+H]$^+$: 457.2598; found:457.2596.

4.2.1.9

*3-Cyano-N-(1-((3S,5R)-4-(cyclopentanecarbonyl)-3,5-dimethylpiperazin-1-yl)-2,3-dihydro-1H-inden-4-yl)benzamide(**4c**)* as white solid (28.5%); mp 101.6-102.7°C. ^{1}H NMR (400 MHz, DMSO-d_6) δ 10.13 (s, 1H), 8.39 (s, 1H), 8.25 (d, J = 8.0 Hz, 1H), 8.08 (d, J = 7.7 Hz, 1H), 7.76 (t, J = 7.8 Hz, 1H), 7.37 (d, J = 7.1 Hz, 1H), 7.27 (t, J = 8 Hz, 1H), 7.23 (d, J = 7.3 Hz, 1H), 4.42 (m, 2H), 4.10 (m, 1H), 2.89-2.83 (m, 2H), 2.79-2.73 (m, 2H), 2.45 (m, 1H), 2.28-2.23 (m, 2H), 1.98 (m, 2H), 1.78-1.50 (m, 8H), 1.39-1.16 (m, 6H). ^{13}C NMR (151 MHz, DMSO-d_6) δ 174.01, 163.12, 144.05, 138.09, 135.47, 134.82, 133.75, 132.36, 131.21, 129.68, 126.51, 123.19, 121.84, 118.16, 111.39, 69.43, 55.58, 50.49, 47.80, 44.18, 30.94, 29.53, 28.45, 25.60, 22.85, 22.03, 21.62, 20.55, 20.16. MS (ESI) m/z: 471.3 [M+H]$^+$. HRMS (ESI$^+$) m/z calcd for $C_{29}H_{34}N_4O_2$ [M+H]$^+$: 471.2755; found:471.2745.

4.2.1.10

*3-Cyano-N-(1-(8-(cyclopentanecarbonyl)-3,8-diazabicyclo [3.2.1] octan-3-yl)-2,3-dihydro-1H-inden-4-yl) benzamide(**4d**)* as white solid (60.4%); mp 115.3-116.4°C. ^{1}H NMR (400 MHz, DMSO-d_6) δ 9.99 (s, 1H), 8.26 (s, 1H), 8.11 (d, J = 7.3 Hz, 1H), 7.95 (d, J = 7.4 Hz, 1H), 7.62 (t, J = 7.5 Hz, 1H), 7.23 (d, J = 7.5 Hz, 1H), 7.13 (t, J = 7.4 Hz, 1H), 7.04 (d, J = 7.2 Hz, 1H), 4.34-4.13(m, 3H), 2.71 (m, 2H), 2.59 (m, 2H), 2.32 (m, 1H), 2.17-2.12 (m, 2H), 1.84 (m, 2H), 1.75-1.36 (m, 12H). ^{13}C NMR (151 MHz, DMSO- d_6) δ 170.85, 163.12, 143.79, 138.03, 135.47, 134.82, 133.74, 132.36, 131.21, 129.68, 126.51, 123.14, 121.89, 118.16, 111.39, 68.21, 56.94, 54.44, 51.69,

50.24, 40.81, 29.77, 29.61, 28.53, 28.32, 26.63, 25.64, 25.56, 23.60. MS (ESI) m/z: 469.3[M+H]$^+$. HRMS (ESI$^+$) m/z calcd for $C_{29}H_{32}N_4O_2$ [M+H]$^+$: 469.2598; found: 469.2593.

4.2.1.11

*3-Cyano-N-(3-(8-(cyclobutanecarbonyl)-3,8-diazabicyclo [3.2.1] octan-3-yl)-2,3-dihydro-1H-inden-5-yl) benzamide(**5a**)* as white solid (55.0%); mp 114.6-115.8°C. ^{1}H NMR (400 MHz, DMSO-d_6) δ 10.38 (s, 1H), 8.39 (s, 1H), 8.24 (d, *J* = 8.0 Hz, 1H), 8.06 (d, *J* = 7.5 Hz, 1H), 7.86-7.68 (m, 2H), 7.67-7.56 (m, 1H), 7.19 (d, *J* = 8.0 Hz, 1H), 4.42 (dd, *J* = 5.6 Hz, 27.9 Hz, 1H), 4.29 (t, *J* = 7.0 Hz, 1H), 4.08, (dd, *J* = 5.0 Hz, 29.1 Hz, 1H), 3.28 (m, 1H), 2.81 (m, 1H), 2.72 (m, 2H), 2.45 (m, 1H), 2.47-2.17 (m, 4H), 2.09-1.63 (m, 10H). ^{13}C NMR (151 MHz, DMSO-d_6) δ 169.31, 163.33, 142.97, 138.74, 137.08, 135.99, 134.68, 132.34, 131.09, 129.62, 124.31, 119.60, 118.18, 116.58, 111.32, 68.08, 57.07, 55.67, 54.01, 51.35, 36.46, 29.59, 28.18, 26.72, 24.63, 24.17, 23.89, 17.48. MS (ESI) m/z: 455.3[M+H]$^+$. HRMS (ESI$^+$) m/z calcd for $C_{28}H_{30}N_4O_2$ [M+H]$^+$: 455.2442; found:455.2433.

4.2.1.12

*3-Cyano-N-(3-(8-(cyclohexanecarbonyl)-3,8-diazabicyclo [3.2.1] octan-3-yl)-2,3-dihydro-1H-inden-5-yl) benzamide(**5b**)* as white solid (45.6%); mp 242.8-243.2°C.^{1}H NMR (400 MHz, DMSO-d_6) δ 10.39 (s, 1H), 8.40 (s, 1H), 8.25 (d, *J* = 7.8 Hz, 1H), 8.07 (d, *J* = 7.8 Hz, 1H), 7.76 (m, 2H), 7.60 (d, *J* = 7.7 Hz, 1H), 7.19 (d, *J* = 8.0 Hz, 1H), 4.44 (dd, *J* = 25.3 Hz, 6.5 Hz, 1H), 4.35-4.22 (m, 2H)., 2.79-2.68 (m, 3H), 2.45 (m, 2H), 2.35-2.21 (m, 2H), 1.98 (m, 2H), 1.89 (m, 2H), 1.67-1.23 (m, 12H). ^{13}C NMR (151 MHz, DMSO-d_6) δ 170.96, 163.32, 142.96, 138.78, 137.08, 135.98, 134.68, 132.34, 131.09, 129.63, 124.32, 119.61, 118.18, 116.62, 111.32, 68.05, 57.24, 55.66, 54.07, 51.20, 40.21, 29.60, 29.23, 29.05, 28.45, 26.68, 25.39, 25.05, 24.94, 24.10. MS (ESI) m/z: 483.3[M+H]$^+$. HRMS (ESI$^+$) m/z calcd for $C_{30}H_{34}N_4O_2$ [M+H]$^+$: 483.2755; found:483.2744.

4.2.1.13

*3-Cyano-N-((3S)-3-(8-(cyclohexanecarbonyl)-3,8-diazabicyclo [3.2.1] octan-3-yl)-2,3 - dihydro-1H-inden-5-yl) benzamide (**5c**)* as white solid (42.0%); mp 110.2-112.5°C. ee: 100%, $[\alpha]_D^{23}$ +122° (c 0.37, $CHCl_3$). ^{1}H NMR (400 MHz, DMSO-d_6) δ 10.39 (s, 1H), 8.40 (s, 1H), 8.25 (d, *J* = 7.8 Hz, 1H), 8.07 (d, *J* = 7.8 Hz, 1H), 7.76 (m, 2H), 7.60 (d, *J* = 7.7 Hz, 1H), 7.19 (d, *J* = 8.0 Hz, 1H), 4.44 (dd, *J* = 25.3 Hz, 6.5 Hz, 1H), 4.35-4.22 (m, 2H)., 2.79-2.68 (m, 3H), 2.45 (m, 2H), 2.35-2.21 (m, 2H), 1.98 (m, 2H), 1.89 (m, 2H), 1.67-1.23 (m, 12H). ^{13}C NMR (151 MHz, DMSO-d_6) δ 170.96, 163.32, 142.96, 138.78, 137.08, 135.98, 134.68, 132.34, 131.09, 129.63, 124.32, 119.61, 118.18, 116.62, 111.32, 68.05, 57.24, 55.66, 54.07, 51.20, 40.21, 29.60, 29.23, 29.05, 28.45, 26.68, 25.39, 25.05, 24.94, 24.10. MS (ESI) m/z: 483.3$[M+H]^+$. HRMS (ESI^+) m/z calcd for $C_{30}H_{34}N_4O_2$ $[M+H]^+$: 483.2755; found:483.2744.

4.2.1.14

*3-Cyano-N-((3R)-3-(8-(cyclohexanecarbonyl)-3,8-diazabicyclo [3.2.1] octan-3-yl) -2,3 -dihydro-1H-inden-5-yl) benzamide (**5d**)* as white solid (56.0%); mp 112.6-113.8°C. ee:100%, $[\alpha]_D^{23}$ -122° (c 0.37, $CHCl_3$). ^{1}H NMR (400 MHz, DMSO-d_6) δ 10.39 (s, 1H), 8.40 (s, 1H), 8.25 (d, *J* = 7.8 Hz, 1H), 8.07 (d, *J* = 7.8 Hz, 1H), 7.76 (m, 2H), 7.60 (d, *J* = 7.7 Hz, 1H), 7.19 (d, *J* = 8.0 Hz, 1H), 4.44 (dd, *J* = 25.3 Hz, 6.5 Hz, 1H), 4.35-4.22 (m, 2H)., 2.79-2.68 (m, 3H), 2.45 (m, 2H), 2.35-2.21 (m, 2H), 1.98 (m, 2H), 1.89 (m, 2H), 1.67-1.23 (m, 12H). ^{13}C NMR (151 MHz, DMSO-d_6) δ 170.96, 163.32, 142.96, 138.78, 137.08, 135.98, 134.68, 132.34, 131.09, 129.63, 124.32, 119.61, 118.18, 116.62, 111.32, 68.05, 57.24, 55.66, 54.07, 51.20, 40.21, 29.60, 29.23, 29.05, 28.45, 26.68, 25.39, 25.05, 24.94, 24.10. MS (ESI) m/z: 483.3$[M+H]^+$. HRMS (ESI^+) m/z calcd for $C_{30}H_{34}N_4O_2$ $[M+H]^+$: 483.2755; found:483.2744.

4.2.1.15

*3-Cyano-N-(3-(8-(2-cyclobutylacetyl)-3,8-diazabicyclo [3.2.1] octan-3-yl)- 2,3-dihydro-1H-inden-5-yl) benzamide(**5e**)* as white solid (42.4%); mp 100.8-101.4°C. ^{1}H NMR (400 MHz, DMSO-d_6) δ 10.39 (s, 1H), 8.40 (s, 1H), 8.24 (d, *J* = 7.2 Hz, 1H), 8.06 (d, *J* = 6.3 Hz, 1H), 7.75 (m, 2H), 7.60 (s, 1H), 7.19 (d, *J* = 7.4 Hz, 1H),

4.44-4.18(m, 3H), 2.76-2.50 (m, 5H), 2.43-2.25 (m, 5H), 1.99-1.63 (m, 11H). ^{13}C NMR (151 MHz, DMSO- d_6) 166.92, 163.33, 142.94, 138.80, 137.08, 135.98, 134.70, 132.35, 131.09, 129.63, 124.33, 119.62, 118.19, 116.62, 111.33, 68.07, 56.79, 55.50, 54.66, 51.38, 31.98, 29.62, 28.38, 27.80, 27.71, 26.70, 26.66, 24.21, 18.04. MS (ESI) m/z: 469.3 $[M+H]^+$. HRMS (ESI^+) m/z calcd for $C_{29}H_{32}N_4O_2$ $[M+H]^+$: 469.2598; found: 469.2592.

4.2.1.16

*N-(3-(8-(Cyclopentanecarbonyl)-3,8-diazabicyclo [3.2.1] octan-3-yl)-2,3-dihydro-1H-inden-5-yl)-6-methylnicotinamide(**5f**)* as white solid (38.4%); mp 228.3-231.2°C. ^{1}H NMR (400 MHz, DMSO-d_6) δ 10.31 (s, 1H), 9.00 (s, 1H), 8.19 (d, J = 7.0 Hz, 1H), 7.78 (d, J = 9.2 Hz, 1H), 7.59 (brs, 1H), 7.42 (d, J = 7.5 Hz, 1H), 7.18 (d, J = 7.5 Hz, 1H), 4.49-4.29(m, 3H), 2.84-2.69 (m, 5H), 2.56 (s, 3H), 2.32 (m, 2H), 1.98-1.50 (m, 14H). ^{13}C NMR (151 MHz, DMSO-d_6) δ 170.88, 163.67, 160.81, 148.03, 142.94, 138.57, 137.25, 135.48, 127.78, 124.27, 122.50, 119.59, 116.58, 68.06, 57.00, 55.65, 54.58, 54.09, 51.37, 50.93, 40.79, 29.77, 29.62, 28.40, 26.70, 25.66, 25.58, 24.10, 23.94. MS (ESI) m/z: 459.3 $[M+H]^+$. HRMS (ESI^+) m/z calcd for $C_{28}H_{34}N_4O_2$ $[M+H]^+$: 459.2755; found: 459.2753.

4.2.1.17

*N-(3-(8-(Cyclopentanecarbonyl)-3,8-diazabicyclo [3.2.1] octan-3-yl)-2,3-dihydro-1H-inden-5-yl)-2-(tetrahydro-2H-pyran-4-yl) acetamide (**5g**)* as white solid (55.6%); mp 89.5-90.2°C. ^{1}H NMR (400 MHz, DMSO-d_6) δ 9.83 (s, 1H), 7.60 (d, J = 14.7 Hz, 1H), 7.40 (t, J = 9.5 Hz, 1H), 7.09 (d, J = 8.1 Hz, 1H), 4.44 (dd, J = 5.9 Hz, 26.2 Hz, 1H), 4.34-4.22 (m, 2H), 3.82 (m, 2H), 3.30 (m, 2H), 2.89-2.62 (m, 4H), 2.43 (m, 1H), 2.31-2.22 (m, 4H), 1.98-1.93 (m, 2H), 1.90-1.50 (m, 14H), 1.27-1.19(m, 3H). ^{13}C NMR (151 MHz, DMSO-d_6) δ 170.76, 169.52, 142.87, 137.55, 124.20, 118.33, 115.33, 68.03, 66.72, 56.94, 55.52, 54.74, 54.46, 54.09, 51.36, 50.93, 50.06, 43.49, 40.79, 32.29, 31.90, 29.77, 29.61, 28.37, 26.67, 25.57, 24.12. MS (ESI) m/z: 466.3 $[M+H]^+$. HRMS (ESI^+) m/z calcd for $C_{28}H_{39}N_3O_3$ $[M+H]^+$: 466.3064; found:

466.3060.

4.2.1.18

*N-(3-(8-(Cyclopentanecarbonyl)-3,8-diazabicyclo[3.2.1]octan-3-yl)-2,3-dihydro -1H - inden-5-yl)-5-fluoro-6-methylnicotinamide(**5h**)* as white solid (56.9%); mp 109.2-110.6°C. ^{1}H NMR (400 MHz, DMSO-d_6) δ 10.36 (s, 1H), 8.86 (s, 1H), 8.13 (d, *J* = 10.4 Hz, 1H), 7.78 (d, *J* = 9.2 Hz, 1H), 7.58 (s, 1H), 7.19 (d, *J* = 8.2 Hz, 1H), 4.45 (dd, *J* = 6.5 Hz, 27 Hz, 1H), 4.34 (m, 2H), 2.90-2.78 (m, 2H), 2.75-2.68 (m, 2H), 2.53 (s, 3H), 2.45 (m, 1H), 2.33-2.25 (m, 2H), 1.99 (m, 2H), 1.92 (m, 2H), 1.72-1.50(m, 10H). ^{13}C NMR (151 MHz, DMSO-d_6) δ 170.78, 162.32, 157.46, 155.77, 143.82, 143.01, 138.83, 136.99, 130.20, 124.33, 121.46, 119.62, 116.60, 68.05, 57.00, 55.67, 54.08, 51.37, 40.79, 29.62, 28.40, 28.24, 26.70, 26.58, 25.64, 24.09, 23.90, 17.79. MS (ESI) m/z: 477.3[M+H]$^{+}$. HRMS (ESI^{+}) m/z calcd for $C_{28}H_{33}FN_4O_2$ [M+H]$^{+}$: 477.2660; found: 477.2656.

4.2.1.19

*1-(3-Cyanophenyl)-3-(3-(8-(cyclopentanecarbonyl)-3,8-diazabicyclo[3.2.1] octan-3 -yl)-2,3-dihydro-1H-inden-5-yl)urea(**5i**)* as white solid (46.9%); mp 139.5-141.2°C.^{1}H NMR (400 MHz, DMSO-d_6) δ 8.93 (s, 1H), 8.80 (s, 1H), 7.94 (m, 1H), 7.64 (d, *J* = 8.2 Hz, 1H), 7.46 (t, J = 7.9 Hz, 2H), 7.40 (t, J = 8.7 Hz, 1H), 7.26-7.16 (m, 1H), 7.09 (d, *J* = 8.0 Hz, 1H), 4.42 (dd, *J* = 5.3 Hz, 23.7 Hz, 1H), 4.32-4.22 (m, 2H), 2.85-2.79 (m, 2H), 2.74-2.63 (m, 2H), 2.40 (m, 1H), 2.30-2.22 (m, 2H), 1.95 (m, 2H), 1.87-1.47(m, 12H). ^{13}C NMR (151 MHz, DMSO-d_6) 170.79, 152.29, 143.08, 140.62, 137.53, 136.94, 130.00, 125.00, 124.45, 122.65, 120.52, 118.74, 117.91, 114.74, 111.42, 68.05, 56.95, 54.74, 54.11, 51.34, 50.10, 40.81, 29.81, 29.60, 28.37, 26.66, 25.64, 24.23. MS (ESI) m/z: 484.3[M+H]$^{+}$. HRMS (ESI^{+}) m/z calcd for $C_{29}H_{33}N_5O_2$ [M+H]$^{+}$: 484.2707; found: 484.2710.

4.2.1.20

*3-Cyano-N-(1-(8-(cyclobutanecarbonyl)-3,8-diazabicyclo [3.2.1] octan-3-yl)-2,3-dihydro-1H-inden-4-yl) benzamide(**6a**)* as white solid (38.1%); mp 105.9-106.7°C.

^{1}H NMR (400 MHz, DMSO-d_6) δ 10.11 (s, 1H), 8.38 (s, 1H), 8.24 (d, *J* = 7.7 Hz, 1H), 8.07 (d, *J* = 7.7 Hz, 1H), 7.75 (t, *J* = 7.8 Hz, 1H, 1H), 7.36 (d, *J* = 7.7 Hz, 1H), 7.25 (t, *J* = 7.6 Hz, 1H), 7.16 (d, *J* = 7.2 Hz, 1H), 4,41 (dd, *J* = 5.5 Hz, 26.2 Hz, 1H), 4.32 (t, *J* = 6.9 Hz, 1H), 4.08 (dd, *J* = 4.3 Hz, 29.6 Hz, 1H), 3.27 (m, 1H), 2.83 (m, 1H), 2.74-2.67 (m, 2H), 2.46-2.38 (m, 1H), 2.27-2.10 (m, 4H), 2.03-1.64 (m, 10H). ^{13}C NMR (151 MHz, DMSO-d_6) δ 169.34, 163.11, 143.72, 138.01, 135.46, 134.81, 133.72, 132.35, 131.21, 129.68, 126.51, 123.13, 121.87, 118.15, 111.39, 68.21, 55.39, 53.60, 51.31, 50.15, 36.47, 28.50, 28.17, 26.64, 24.68, 24.13, 23.55, 17.48. MS (ESI) m/z: 455.3[M+H]$^+$. HRMS (ESI$^+$) m/z calcd for $C_{28}H_{30}N_4O_2$ [M+H]$^+$: 455.2442; found:455.2442.

4.2.1.21

*3-Cyano-N-(1-(8-(cyclohexanecarbonyl)-3,8-diazabicyclo [3.2.1] octan-3-yl)-2,3 -dihydro-1H-inden-4-yl) benzamide (**6b**)* as white solid (46.5%); mp 118.1-119.6°C. ^{1}H NMR (400 MHz, DMSO-d_6) δ 10.11 (s, 1H), 8.38 (s, 1H), 8.24 (d, *J* = 7.5 Hz, 1H), 8.07 (d, *J* = 7.6 Hz, 1H), 7.75 (t, *J* = 7.6 Hz, 1H, 1H), 7.36 (d, *J* = 7.7 Hz, 1H), 7.26 (t, *J* = 7.3 Hz, 1H), 7.17 (d, *J* = 6.7 Hz, 1H), 4,43 (dd, *J* = 4.8 Hz, 25.3 Hz, 1H), 4.36 -4.20 (m, 2H), 2.83 (m, 1H), 2.78-2.67 (m, 2H), 2.43 (m, 2H), 2.34-2.25 (m, 2H), 1.97-1.62 (m, 11H), 1.38-1.10 (m, 5H). ^{13}C NMR (151 MHz, DMSO-d_6) δ 170.91, 163.11, 143.76, 138.06, 135.47, 134.82, 133.73, 132.36, 131.21, 129.68, 126.51, 123.14, 121.91, 118.16, 111.39, 68.20, 57.12, 55.50, 54.41, 54.06, 51.14, 50.70, 40.21, 29.23, 28.56, 28.37, 26.62, 25.38, 25.05, 23.66. MS (ESI) m/z: 483.3[M+H]$^+$. HRMS (ESI$^+$) m/z calcd for $C_{30}H_{34}N_4O_2$ [M+H]$^+$: 483.2755; found:483.2759.

4.2.1.22

*3-Cyano-N-(1-(8-(2-cyclobutylacetyl)-3,8-diazabicyclo[3.2.1]octan-3-yl)-2,3-dihydro -1H-inden-4-yl)benzamide (**6c**)* as white solid (56.5%); mp 187.4-189.1°C. ^{1}H NMR (400 MHz, DMSO-d_6) δ 10.11 (s, 1H), 8.38 (s, 1H), 8.24 (d, *J* = 7.7 Hz, 1H), 8.07 (d, *J* = 7.6 Hz, 1H), 7.75 (t, *J* = 7.8 Hz, 1H), 7.36 (d, *J* = 7.8 Hz, 1H), 7.25 (t, *J* = 7.5 Hz, 1H), 7.17 (d, *J* = 7.0 Hz, 1H), 4.42 (dd, *J* = 4.7 Hz, 24.6 Hz, 1H), 4.33 (t, *J* = 6.9 Hz, 1H), 4.22 (dd, *J* = 4.5 Hz, 31.3 Hz, 1H), 2.82 (m, 1H), 2.74 (m, 1H), 2.68 (m, 1H),

2.58 (m, 1H), 2.47-2.24 (m, 6H), 2.00-1.59 (m, 11H). ^{13}C NMR (151 MHz, DMSO-d_6) δ 166.88, 163.11, 143.73, 138.02, 135.53, 134.81, 133.72, 132.35, 131.21, 129.68, 126.50, 123.13, 121.89, 118.15, 111.39, 68.22, 55.43, 54.26, 51.27, 50.87, 32.01, 28.51, 28.31, 27.80, 26.64, 23.65, 18.04. MS (ESI) m/z: 469.3[M+H]$^+$. HRMS (ESI$^+$) m/z calcd for $C_{29}H_{32}N_4O_2$ [M+H]$^+$: 469.2598; found:469.2594.

4.2.1.23

*N-(1-(8-(Cyclopentanecarbonyl)-3,8-diazabicyclo[3.2.1]octan-3-yl)-2,3-dihydro-1H-inden-4-yl)-6-methylnicotinamide(**6d**)* as white solid (44.5%); mp 99.0-101.2°C. ^{1}H NMR (400 MHz, DMSO-d_6) δ 10.02 (s, 1H), 8.99 (s, 1H), 8.18 (d, J = 8.1 Hz, 1H), 7.41 (t, J = 8.1 Hz, 1H), 7.36 (d, J = 7.7 Hz, 1H), 7.25 (t, J = 7.5 Hz, 1H), 7.16 (d, J = 7.3 Hz, 1H), 4.44 (dd, J = 6.1 Hz, 26.0 Hz, 1H), 4.35-4.26 (m, 2H), 2.85 (m, 2H), 2.72 (m, 2H), 2.55 (s, 3H), 2.44 (t, J = 8 Hz, 1H), 2.32-2.25 (m, 2H), 1.97 (m, 2H), 1.90-1.78 (m, 2H), 1.73-1.49(m, 10H). ^{13}C NMR (151 MHz, DMSO-d_6) δ 170.80, 163.46, 160.98, 148.12, 143.68, 138.00, 135.52, 133.88, 127.24, 126.47, 123.17, 122.55, 121.73, 68.23, 55.46, 54.07, 51.32, 50.24, 40.81, 29.61, 28.52, 28.32, 26.63, 25.56, 23.94, 23.60. MS (ESI) m/z: 459.3 [M+H]$^+$. HRMS (ESI$^+$) m/z calcd for $C_{28}H_{34}N_4O_2$ [M+H]$^+$: 459.2755; found:459.2751.

4.2.1.24

*N-(1-(8-(Cyclopentanecarbonyl)-3,8-diazabicyclo[3.2.1]octan-3-yl)-2,3-dihydro-1H-inden-4-yl)-2-(tetrahydro-2H-pyran-4-yl)acetamide(**6e**)* as white solid (46.5%); mp 85.6-86.0°C. ^{1}H NMR (400 MHz, DMSO-d_6) δ 9.28 (s, 1H), 7.44 (d, J = 8.2 Hz, 1H), 7.19-7.11 (m, 1H), 7.04 (d, J = 6.2 Hz, 1H), 4.41 (m, 1H), 4.33-4.16 (m, 2H), 3.82 (m, 2H), 3.29 (m, 2H), 2.84-2.71 (m, 2H), 2.66-2.63 (m, 2H), 2.43-2.39 (m, 1H), 2.26-2.21 (m, 4H), 1.95 (m, 2H), 1.84-1.50 (m, 14H), 1.29-1.19(m, 3H). ^{13}C NMR (151 MHz, DMSO-d_6) δ 170.83, 169.57, 143.46, 135.70, 134.33, 126.39, 121.46, 120.63, 68.21, 66.73, 56.96, 56.88, 55.49, 54.42, 51.30, 50.90, 42.86, 40.80, 32.24, 29.61, 28.31, 26.62, 25.63, 23.53. MS (ESI) m/z: 466.3 [M+H]$^+$. HRMS (ESI$^+$) m/z calcd for $C_{28}H_{39}N_3O_3$ [M+H]$^+$: 466.3064; found: 466.3068.

4.2.1.25

*N-(1-(8-(Cyclopentanecarbonyl)-3,8-diazabicyclo [3.2.1] octan-3-yl)-2,3-dihydro-1H-inden-4-yl)-5-fluoro-6-methylnicotinamide(**6f**)* as white solid (46.5%); mp 107.8-108.9°C. ^{1}H NMR (400 MHz, DMSO-d_6) δ 10.11 (s, 1H), 8.86 (s, 1H), 8.10 (d, J = 10.2 Hz, 1H), 7.35 (d, J = 6.9 Hz, 1H), 7.26 (t, J = 7.8 Hz, 1H), 7.17 (d, J = 6.9 Hz, 1H), 4.43 (m, 1H), 4.33-4.26 (m, 2H), 2.82 (m, 2H), 2.75-2.68 (m, 2H), 2.53 (s, 3H), 2.45 (m, 1H), 2.29-2.25 (m, 2H), 1.97 (m, 2H), 1.88 (m, 2H), 1.71-1.49(m, 10H). ^{13}C NMR (151 MHz, DMSO-d_6) 170.80, 162.13, 157.49, 155.76, 149.08, 143.86, 138.06, 133.59, 129.69, 126.53, 123.18, 121.95, 121.49, 71.19, 68.20, 56.93, 55.45, 54.06, 51.31, 50.25, 40.80, 29.61, 28.53, 28.32, 26.62, 25.56, 23.62, 17.80. MS (ESI) m/z: 477.3[M+H]$^+$. HRMS (ESI$^+$) m/z calcd for $C_{28}H_{33}FN_4O_2$ [M+H]$^+$: 477.2660; found: 477.2653.

4.2.1.26

*1-(3-Cyanophenyl)-3-(1-(8-(cyclopentanecarbonyl)-3,8 –diazabicyclo [3.2.1] octan -3 -yl)-2,3-dihydro-1H-inden-4-yl) urea(**6g**)* as white solid (66.5%); mp 142.7-143.4°C. ^{1}H NMR (400 MHz, DMSO-d_6) δ 9.34 (s, 1H), 8.19 (s, 1H), 8.03 (s, 1H), 7.83 (s, 1H), 7.64 (s, 1H), 7.51 (s, 1H), 7.45 (s, 1H), 7.19 (s, 1H), 6.99 (s, 1H), 4.42 (m, 1H), 4.32-4.22 (m, 2H), 2.85-2.79 (m, 2H), 2.74-2.63 (m, 2H), 2.45 (m, 1H), 2.29 (m, 2H), 1.99 (m, 2H), 1.74-1.52(m, 12H). ^{13}C NMR (151 MHz, DMSO-d_6) 170.84, 152.14, 143.31, 140.47, 135.08, 132.51, 130.08, 126.84, 125.12, 122.51, 120.36, 118.91, 118.70, 117.92, 111.51, 68.29, 56.80, 54.74, 54.07, 51.30, 40.80, 29.75, 28.31, 27.81, 26.63, 25.64, 23.51. MS (ESI) m/z: 484.3[M+H]$^+$. HRMS (ESI$^+$) m/z calcd for $C_{29}H_{33}N_5O_2$ [M+H]$^+$: 484.2707; found: 484.2703.

4.3. Biological assays

4.3.1. RORγ FRET assay

The assays were performed in an assay buffer consisting of 50 mM NaF, 50 mM 3-(*N*-morpholino)propanesulfonic acid, pH 7.4, 0.05 mM 3-[(3-cholamidopropyl) dimethylammonio]propanesulfonate, 0.1 mg/mL bovine serum albumin, and 10 mM

dithiothreitol in 384-well plates. The total volume was 25 μL/well. The europium-labeled SRC1 solution was prepared by adding an appropriate amount of biotinylated SRC and europium labeled streptavidin into assay buffer, with final concentrations of 20 and 10 nM, respectively. The allophycocyanin (APC)-labeled-LBD solution was prepared by adding an appropriate amount of biotinylated RORc-LBD and APC-labeled streptavidin at final concentrations of 20 and 10 nM, respectively. After 15 min of incubation at room temperature, a 20-fold excess of biotin was added and incubated for 10 min at room temperature to block the remaining free streptavidin. Equal volumes of europium-labeled SRC and APC-labeled RORc-LBD were then mixed with 0.1 μM surrogate agonist *N*-(2-chloro-6-fluorobenzyl)-*N*-((20-methoxy-[1,10-biphenyl]-4-yl) methyl) benzenesulfonamide and dispensed into 384-well assay plates at 25 μL volume/well. The 384-well assay plates had 100 nL of test compound in DMSO predispensed into each well. The plates were incubated for 1 h at room temperature and then read on Envision in LANCE mode configured for europeum-APC labels.

4.3.2. Mouse Th17 differentiation assay

$CD4^+$ T cells were purified from mouse splenocytes using a commercial $CD4^+$ T cell negative selection kit (Invitrogen). $CD4^+$ T cells were skewed to Th17 cells by culturing cells in the presence of anti-CD3 (0.25 μg/mL, Bioxcel), anti-CD28 (1 μg/mL, Bioxcel), anti-IFN-γ (2 μg/mL, Bioxcel), anti-IL-4 (2 μg/mL, Bioxcel), TGF-β (5 ng/mL, Peprotech) and IL-6 (20 ng/mL, Peprotech) for 4 days before analysis. Compounds or DMSO control were added to the culture on day 0 of Th17 differentiation at indicated concentrations. Percentage of IL-17 production from $CD4^+$ T cells were analyzed by intracellular staining followed by flow cytometry. Dose-response curves were plotted to determine half-maximal inhibitory concentrations (IC_{50}) for the compounds using the GraphPad Prism 5 (GraphPad Software, San Diego CA, USA).

4.3.3. Molecular docking studies

Molecular docking was carried out using Schrodinger 3.5 software package. The co-crystal structure of RORγt LBD (PDB: 6CN6) was selected and processed using the Protein Preparation Wizard including water deletion, addition of missing hydrogen

atoms as well as adjustment of the tautomerization and protonation states of histidine. The compound 3D structures were subjected to energy minimization with force field (OPLS_2005) before submitting to the docking procedure. The docking grid was centered according to the ligand position, and the bounding box was set to 15 Å. This docking was performed with Glide-docking using Extra Precision (GlideXP) algorithm. The final ranking from the docking was based on the docking score, which combines the Epik state penalty with the Glide Score. High-scoring complexes were inspected visually to select the most reasonable solution.

Acknowledgements

This work was supported by National Science Foundation of China (Grant Numbers: 81573276 and 81874287), Shanghai Bio-pharmaceutical Science and Technology Supporting Plan (Grant Number: 17431902100), National Science & Technology Major Project "Key New Drug Creation and Manufacturing Program" of China (Grant Number：2018ZX09711002) and Fudan-SIMM Joint Research Fund (Grant Number: FU-SIMM20174007).

Appendix A. Supplementary data

Supplementary data related to this article can be found at https://doi.org/10.1016/j.ejmech.2018.02.050.

References

[1] Y.W. He, M.L. Deftos, E.W. Ojala, M.J. Bevan. RORγt, a Novel Isoform of an Orphan Receptor, Negatively Regulates Fas Ligand Expression and IL-2 Production in T Cells, Immunity. 9 (1998) 797-806.

[2] T. Hirose, R.J. Smith, A.M. Jetten. ROR-γ: The Third Member of ROR/RZR Orphan Receptor Subfamily That Is Highly Expressed in Skeletal Muscle, Biochemical and Biophysical Research Communications. 205 (1994) 1976-1983.

[3] F. Annunziato, L. Cosmi, V. Santarlasci, L. Maggi, F. Liotta, B. Mazzinghi, E. Parente, L. Fili, S. Ferri, F. Frosali, F. Giudici, P. Romagnani, P. Parronchi, F. Tonelli, E. Maggi, S. Romagnani.

Phenotypic and functional features of human Th17 cells, J Exp Med. 204 (2007) 1849-1861.

[4] I.I. Ivanov, B.S. McKenzie, L. Zhou, C.E. Tadokoro, A. Lepelley, J.J. Lafaille, D.J. Cua, D.R. Littman. The Orphan Nuclear Receptor RORγt Directs the Differentiation Program of Proinflammatory IL-17+ T Helper Cells, Cell. 126 (2006) 1121-1133.

[5] A.M. Jetten. Retinoid-related orphan receptors (RORs): critical roles in development, immunity, circadian rhythm, and cellular metabolism, Nucl Recept Signal. 7 (2009) e003.

[6] V. Giguere, M. Tini, G. Flock, E. Ong, R.M. Evans, G. Otulakowski. Isoform-specific amino-terminal domains dictate DNA-binding properties of ROR alpha, a novel family of orphan hormone nuclear receptors, Genes & Development. 8 (1994) 538-553.

[7] R.H. Duerr, K.D. Taylor, S.R. Brant, J.D. Rioux, M.S. Silverberg, M.J. Daly, A.H. Steinhart, C. Abraham, M. Regueiro, A. Griffiths, T. Dassopoulos, A. Bitton, H. Yang, S. Targan, L.W. Datta, E.O. Kistner, L.P. Schumm, A.T. Lee, P.K. Gregersen, M.M. Barmada, J.I. Rotter, D.L. Nicolae, J.H. Cho. A Genome-Wide Association Study Identifies IL23R as an Inflammatory Bowel Disease Gene, Science. 314 (2006) 1461.

[8] C.M. Wilke, K. Bishop, D. Fox, W. Zou. Deciphering the role of Th17 cells in human disease, Trends Immunol. 32 (2011) 603-611.

[9] P. Miossec, J.K. Kolls. Targeting IL-17 and TH17 cells in chronic inflammation, Nature Reviews Drug Discovery. 11 (2012) 763-776.

[10] A. Beringer, M. Noack, P. Miossec. IL-17 in Chronic Inflammation: From Discovery to Targeting, Trends in molecular medicine. 22 (2016) 230-241.

[11] M. Campa, B. Mansouri, R. Warren, A. Menter. A Review of Biologic Therapies Targeting IL-23 and IL-17 for Use in Moderate-to-Severe Plaque Psoriasis, Dermatology and therapy. 6 (2016) 1-12.

[12] H. Kebir, I. Ifergan, J.I. Alvarez, M. Bernard, J. Poirier, N. Arbour, P. Duquette, A. Prat. Preferential recruitment of interferon-gamma-expressing TH17 cells in multiple sclerosis, Ann Neurol. 66 (2009) 390-402.

[13] S. Kotake, N. Udagawa, N. Takahashi, K. Matsuzaki, K. Itoh, S. Ishiyama, S. Saito, K. Inoue, N. Kamatani, M.T. Gillespie, T.J. Martin, T. Suda. IL-17 in synovial fluids from patients with

rheumatoid arthritis is a potent stimulator of osteoclastogenesis, The Journal of clinical investigation. 103 (1999) 1345-1352.

[14] L. Rovedatti, T. Kudo, P. Biancheri, M. Sarra, C.H. Knowles, D.S. Rampton, G.R. Corazza, G. Monteleone, A. Di Sabatino, T.T. MacDonald. Differential regulation of interleukin 17 and interferon production in inflammatory bowel disease, Gut. 58 (2009) 1629-1636.

[15] W. Hueber, D.D. Patel, T. Dryja, A.M. Wright, I. Koroleva, G. Bruin, C. Antoni, Z. Draelos, M.H. Gold, P. Durez, P.P. Tak, J.J. Gomez-Reino, C.S. Foster, R.Y. Kim, C.M. Samson, N.S. Falk, D.S. Chu, D. Callanan, Q.D. Nguyen, K. Rose, A. Haider, F. Di Padova. Effects of AIN457, a Fully Human Antibody to Interleukin-17A, on Psoriasis, Rheumatoid Arthritis, and Uveitis, Science Translational Medicine. 2 (2010) 52-72.

[16] H. Kellner. Targeting interleukin-17 in patients with active rheumatoid arthritis: rationale and clinical potential, Therapeutic Advances in Musculoskeletal Disease. 5 (2013) 141-152.

[17] C. Leonardi, R. Matheson, C. Zachariae, G. Cameron, L. Li, E. Edson-Heredia, D. Braun, S. Banerjee. Anti–Interleukin-17 Monoclonal Antibody Ixekizumab in Chronic Plaque Psoriasis, New England Journal of Medicine. 366 (2012) 1190-1199.

[18] K.A. Papp, C. Leonardi, A. Menter, J.-P. Ortonne, J.G. Krueger, G. Kricorian, G. Aras, J. Li, C.B. Russell, E.H.Z. Thompson, S. Baumgartner. Brodalumab, an Anti–Interleukin-17–Receptor Antibody for Psoriasis, New England Journal of Medicine. 366 (2012) 1181-1189.

[19] D. Baeten, X. Baraliakos, J. Braun, J. Sieper, P. Emery, D. van der Heijde, I. McInnes, J.M. van Laar, R. Landewé, P. Wordsworth, J. Wollenhaupt, H. Kellner, J. Paramarta, J. Wei, A. Brachat, S. Bek, D. Laurent, Y. Li, Y.A. Wang, A.P. Bertolino, S. Gsteiger, A.M. Wright, W. Hueber. Anti-interleukin-17A monoclonal antibody secukinumab in treatment of ankylosing spondylitis: a randomised, double-blind, placebo-controlled trial, The Lancet. 382 (2013) 1705-1713.

[20] R.G. Langley, B.E. Elewski, M. Lebwohl, K. Reich, C.E. Griffiths, K. Papp, L. Puig, H. Nakagawa, L. Spelman, B. Sigurgeirsson, E. Rivas, T.F. Tsai, N. Wasel, S. Tyring, T. Salko, I. Hampele, M. Notter, A. Karpov, S. Helou, C. Papavassilis, E.S. Group, F.S. Group. Secukinumab in plaque psoriasis--results of two phase 3 trials, The New England journal of medicine. 371 (2014) 326-338.

[21] Y. Zhang, X. Luo, D. Wu, Y. Xu. ROR nuclear receptors: structures, related diseases, and drug discovery, Acta Pharmacol Sin. 36 (2015) 71-87

[22] J.R. Huh, M.W.L. Leung, P.X. Huang, D.A. Ryan, M.R. Krout, R.R.V. Malapaka, J. Chow, N. Manel, M. Ciofani, S.V. Kim, A. Cuesta, F.R. Santori, J.J. Lafaille, H.E. Xu, D.Y. Gin, F. Rastinejad, D.R. Littman. Digoxin and its derivatives suppress T(H)17 cell differentiation by antagonizing ROR gamma t activity, Nature. 472 (2011) 486-490.

[23] L.A. Solt, N. Kumar, P. Nuhant, Y. Wang, J.L. Lauer, J. Liu, M.A. Istrate, T.M. Kamenecka, W.R. Roush, D. Vidovic, S.C. Schurer, J. Xu, G. Wagoner, P.D. Drew, P.R. Griffin, T.P. Burris. Suppression of TH17 differentiation and autoimmunity by a synthetic ROR ligand, Nature. 472 (2011) 491-494.

[24] T. Xu, X. Wang, B. Zhong, R.I. Nurieva, S. Ding, C. Dong. Ursolic acid suppresses interleukin-17 (IL-17) production by selectively antagonizing the function of RORgamma t protein, J Biol Chem. 286 (2011) 22707-22710.

[25] S.M. Bronner, J.R. Zbieg, J.J. Crawford. RORγ antagonists and inverse agonists: a patent review, Expert Opinion on Therapeutic Patents. 27 (2017) 101-112.

[26] V.B. Pandya, S. Kumar, Sachchidanand, R. Sharma, R.C. Desai. Combating Autoimmune Diseases With Retinoic Acid Receptor-Related Orphan Receptor-gamma (RORgamma or RORc) Inhibitors: Hits and Misses, J Med Chem. (2018) DOI: 10.1021/acs. jmedchem. 8b00588

[27] P. Cyr, S.M. Bronner, J.J. Crawford. Recent progress on nuclear receptor RORγ modulators, Bioorganic & Medicinal Chemistry Letters. 26 (2016) 4387-4393.

[28] B.P. Fauber, S. Magnuson. Modulators of the Nuclear Receptor Retinoic Acid Receptor-Related Orphan Receptor-γ (RORγ or RORc), Journal of Medicinal Chemistry. 57 (2014) 5871-5892.

[29] Information from Pharmaprojects, infama database, https://citeline.informa.com/?query=eJyrVkrMyfFPU7KKrkZm5VVCWZnFSlbVSql5JZkllUpWSilFpelKOkp5ibmpUF5IYlF6aokfSEBHqSwxpxQkEeQf5K5UWxuro5ScX1qQk1oCMgSqqQSsoRgkDYQAqyArKA%3D%3D#/drugs. (2018), (accessed 12 December 2018).

[30] Y. Huang, M. Yu, N. Sun, T. Tang, F. Yu, X. Song, Q. Xie, W. Fu, L. Shao, Y. Wang.

Discovery of carbazole carboxamides as novel RORgammat inverse agonists, Eur J Med Chem. 148 (2018) 465-476.

[31] Y. Wang, W. Cai, G. Zhang, T. Yang, Q. Liu, Y. Cheng, L. Zhou, Y. Ma, Z. Cheng, S. Lu, Y.-G. Zhao, W. Zhang, Z. Xiang, S. Wang, L. Yang, Q. Wu, L.A. Orband-Miller, Y. Xu, J. Zhang, R. Gao, M. Huxdorf, J.-N. Xiang, Z. Zhong, J.D. Elliott, S. Leung, X. Lin. Discovery of novel N-(5-(arylcarbonyl)thiazol-2-yl)amides and N-(5-(arylcarbonyl)thiophen-2-yl)amides as potent RORγt inhibitors, Bioorganic & Medicinal Chemistry. 22 (2014) 692-702.

[32] Y. Wang, T. Yang, Q. Liu, Y. Ma, L. Yang, L. Zhou, Z. Xiang, Z. Cheng, S. Lu, L.A. Orband-Miller, W. Zhang, Q. Wu, K. Zhang, Y. Li, J.-N. Xiang, J.D. Elliott, S. Leung, F. Ren, X. Lin. Discovery of N-(4-aryl-5-aryloxy-thiazol-2-yl)-amides as potent RORγt inverse agonists, Bioorganic & Medicinal Chemistry. 23 (2015) 5293-5302.

[33] T. Yang, Q. Liu, Y. Cheng, W. Cai, Y. Ma, L. Yang, Q. Wu, L.A. Orband-Miller, L. Zhou, Z. Xiang, M. Huxdorf, W. Zhang, J. Zhang, J.-N. Xiang, S. Leung, Y. Qiu, Z. Zhong, J.D. Elliott, X. Lin, Y. Wang. Discovery of Tertiary Amine and Indole Derivatives as Potent RORγt Inverse Agonists, ACS Medicinal Chemistry Letters. 5 (2013) 65-68.

[34] Y. Wang, W. Cai, Y. Cheng, T. Yang, Q. Liu, G. Zhang, Q. Meng, F. Han, Y. Huang, L. Zhou, Z. Xiang, Y.-G. Zhao, Y. Xu, Z. Cheng, S. Lu, Q. Wu, J.-N. Xiang, J.D. Elliott, S. Leung, F. Ren, X. Lin. Discovery of Biaryl Amides as Potent, Orally Bioavailable, and CNS Penetrant RORγt Inhibitors, ACS Medicinal Chemistry Letters. (2015) 787-792.

[35] H. Lei, X. Ma, F. Ren, X. Lin, R.W. Marquis, Jr. N-Acylpiperazine derivatives as RORγ modulators and their preparation, WO2015180614A1, 2015.

[36] J. Deng, H. Lei, X. Ma, F. Ren, W. Cai, X. Lin. Preparation of piperazine derivatives as RORγ modulators, WO2015180613A1, 2015.

[37] J. Deng, H. Lei, X. Ma, X. Lin. Acylpiperazine-acylaniline compounds as RORγ modulators and their preparation, pharmaceutical compositions and use in the treatment of inflammatory and autoimmune diseases, WO2015180612A1, 2015.

[38] F. Han, H. Lei, X. Lin, Q. Meng, Y. Wang. Preparation of piperazinylmethylphenyl-substituted caboxamides as modulators of the retinoid-related orphan receptor gamma for use in the treatment of autoimmune and inflammatory diseases,

WO2014086894A1, 2014.

[39] M.E. Schnute, M. Wennerstal, J. Alley, M. Bengtsson, J.R. Blinn, C.W. Bolten, T. Braden, T. Bonn, B. Carlsson, N. Caspers, M. Chen, C. Choi, L.P. Collis, K. Crouse, M. Farnegardh, K.F. Fennell, S. Fish, A.C. Flick, A. Goos-Nilsson, H. Gullberg, P.K. Harris, S.E. Heasley, M. Hegen, A.E. Hromockyj, X. Hu, B. Husman, T. Janosik, P. Jones, N. Kaila, E. Kallin, B. Kauppi, J.R. Kiefer, J. Knafels, K. Koehler, L. Kruger, R.G. Kurumbail, R.E. Kyne, Jr., W. Li, J. Lofstedt, S.A. Long, C.A. Menard, S. Mente, D. Messing, M.J. Meyers, L. Napierata, D. Noteberg, P. Nuhant, M.J. Pelc, M.J. Prinsen, P. Rhonnstad, E. Backstrom-Rydin, J. Sandberg, M. Sandstrom, F. Shah, M. Sjoberg, A. Sundell, A.P. Taylor, A. Thorarensen, J.I. Trujillo, J.D. Trzupek, R. Unwalla, F.F. Vajdos, R.A. Weinberg, D.C. Wood, L. Xing, E. Zamaratski, C.W. Zapf, Y. Zhao, A. Wilhelmsson, G. Berstein. Discovery of 3-Cyano-N-(3-(1-isobutyrylpiperidin-4-yl)-1-methyl-4-(trifluoromethyl)-1 H-pyrrolo[2,3-b]pyridin-5-yl)benzamide: A Potent, Selective, and Orally Bioavailable Retinoic Acid Receptor-Related Orphan Receptor C2 Inverse Agonist, J Med Chem. (2018) DOI: 10.1021/acs.jmedchem.1028b00392.

[40] S. Hintermann, C. Guntermann, H. Mattes, D.A. Carcache, J. Wagner, A. Vulpetti, A. Billich, J. Dawson, K. Kaupmann, J. Kallen, R. Stringer, D. Orain. Synthesis and Biological Evaluation of New Triazolo- and Imidazolopyridine RORγt Inverse Agonists, ChemMedChem. 11 (2016) 2640-2648.

[41] A.S. Jessiman, P.S. Johnson, K. Maansson, M.D. Soerensen. Heteroaromatic compounds as modulators of the retinoid-related orphan receptor gamma and their preparation, WO2018011201A1, 2018.

Research highlights

- Novel *N*-indanyl benzamide derivatives were discovered as potent RORγt inverse agonists.
- The structure-activity relationships (SAR) were explored.
- **5c** as (*S*)-enantiomer showed good RORγt inverse agonist activities in both FRET and mouse Th17 cell differentiation assays.
- The binding mode study demonstrated the superiority of conformational restriction in *N*-indanyl benzamide (*S*)-enantiomers.